HHS Public Access

Author manuscript

Proteomics. Author manuscript; available in PMC 2015 July 24.

Published in final edited form as:

Proteomics. 2012 November ; 12(22): 3343–3364. doi:10.1002/pmic.201200211.

Proteome variation among *Filifactor alocis* strains

A. Wilson Aruni, **Francis Roy**, **Lawrence Sandberg**, and **Hansel M. Fletcher**

Division of Microbiology and Molecular Genetics, School of Medicine, Loma Linda University, Loma Linda, CA, USA

Abstract

Filifactor alocis, a Gram-positive anaerobic rod, is now considered one of the marker organisms associated with periodontal disease. Although there was heterogeneity in its virulence potential, this bacterium was shown to have virulence properties that may enhance its ability to survive and persist in the periodontal pocket. To gain further insight into a possible mechanism(s) of pathogenesis, the proteome of *F. alocis* strains was evaluated. Proteins including several proteases, neutrophil-activating protein A and calcium-binding acid repeat protein, were identified in *F. alocis*. During the invasion of HeLa cells, there was increased expression of several of the genes encoding these proteins in the potentially more virulent *F. alocis* D-62D compared to *F. alocis ATCC* 35896, the type strain. A comparative protein in silico analysis of the proteome revealed more cell wall anchoring proteins in the *F. alocis* D-62D compared to *F. alocis ATCC* 35896. Their expression was enhanced by coinfection with *Porphyromonas gingivalis.* Taken together, the variation in the pathogenic potential of the *F. alocis* strains may be related to the differential expression of several putative virulence factors.

Keywords

Filifactor alocis; Microbiology; Proteases; Proteome; Virulence

1 Introduction

Periodontal disease is associated with a complex microbial milieu harboring several pathogens that can initiate or directly contribute to host tissue destruction. Bacteria such as *Porphyromonas gingivalis, Prevotella intermedia, Aggregatibacter* (*Actinobacillus*) *actinomycetemcomitans, Tannerella forsythia,* and *Treponema denticola* have previously been demonstrated to be major pathogens associated with periodontal diseases [1–3]. A paradigm shift for infection-induced periodontal diseases based on data emerging from the oral microbiome project now suggest the involvement of as-yet-culturable and fastidious organisms [4–7]. Collectively, these studies have demonstrated that there are changes in the periodontal status associated with shifts in the composition of the bacterial community in the periodontal pocket [8, 9].

Correspondence: Dr. H. M. Fletcher, Division of Microbiology and Molecular Genetics, School of Medicine, Loma Linda University, Loma Linda, CA 92350, USA, hfletcher@llu.edu, Fax: +1-909-558-4035.

Colour Online: See the article online to view Figs. 3–6 in colour.

The authors have declared no conflict of interest.

Filifactor alocis (*F. alocis*), a Gram-positive, assacharolytic, obligate anaerobic rod, is one of the marker organisms that is now identified to be significant to the pathogenetic structure of biofilms associated with periodontal inflammation and is suggested to be an important organism for periodontal disease [10–12]. Further, in comparison to the other traditional periodontal pathogens, *F. alocis* is present in the periodontal pocket in higher numbers and is least detected in healthy or periodontitis-resistant patients [13–15]. This organism first isolated in 1985 from the gingival sulcus in gingivitis and periodontis patients was classified as *Fusobacterium alocis* [16]. However, based on phylogenetic analysis using 16s rRNA sequences, it was reclassified in 1999 into the genus *Filifactor* [17].

In a previous report, we have demonstrated that *F. alocis* has virulence properties that may enhance its ability to survive and persist in the periodontal pocket [18]. *F. alocis* was relatively resistant to oxidative stress and its growth was stimulated under those conditions [18]. In addition, as reported elsewhere, there is evidence that the secretion of proinflammatory cytokines, including IL-1β, IL-6, and TNF-α from gingival epithelial cells and apoptosis of these cells can be induced by *F. alocis* [19]. A comparative analysis of several *F. alocis* isolates showed heterogeneity in their virulence potential [18]. Further, in coculture with *P. gingivalis*, these *F. alocis* strains showed variations in their invasive capacity of epithelial cells [18]. While synergistic interactions during polymicrobial infections have resulted in enhanced pathogenesis of periodontopathogens such as *P. gingivalis* [20], a mechanism(s) for *F. alocis* is unclear. It is likely that surface and secretory proteins from *F. alocis* may play a role in this process.

Proteome analyses have contributed significantly toward a deeper understanding of the molecular mechanisms of invasion, adaptation, survival, and pathogenesis in several oral pathogens such as *Streptococcus mutants* [21] *Streptococcus oralis* [22], *Fusobacterium nucleatum* [23], and *P. gingivalis* [24]. In this report, we have evaluated the proteome of *F. alocis ATCC* 35896 and a potentially more virulent strain designated *F. alocis* D-62D. Our comparative analysis revealed variation in several hypothetical proteins and those known to be important virulence factors in other bacteria. Several proteases identified in the proteome of *F. alocis* D-62D were missing in *F. alocis ATCC* 35896. There was differential expression of the genes encoding these proteins during the infection of HeLa cells.

2 Materials and methods

2.1 Bioinformatics analysis

The DNA and amino acid sequences were aligned using Bioedit (http://www.mbio.ncsu.edu/bioedit/bioedit.html). The phylogenetic relationship of these sequences between the oral pathogens was analyzed using MEGA version 4.0 [25]. The signal peptide and potential cleavage sites were predicted using both Neural network and Hidden Markov Model [26]. Metabolic pathway analysis was carried out using the Kyoto Encyclopedia of Genes and Genomes (www.genome.jp/kegg/) [27]. Signal peptide prediction and cleavage site prediction were performed using Signal P 3.0 [28]. Transmembrane helices were predicted using the TMHMM server [29]. The presence of LysM domains, peptidoglycan-binding domains, and choline-binding domains were determined by screening against the Pfam database [30] (E value cutoff of $<1 \times 10^{-5}$). Lipoprotein predictions were performed as

previously described [31]. The sorting motifs and WxL motifs were searched using string search and the results were screened manually determining the motif sequences. Sortase substrates were identified by manual screening and a Hidden Markov model [32].

2.2 Bacterial strains and growth conditions

F. alocis ATCC 35896 was purchased form the American Type Culture Collection (Rockville, MD, USA). *F. alocis* D-62D was a gift from Dr. Floyd Dewhirst, the custodian of the Moores' anaerobic microbial collection (The Forsyth Institute, Boston, MA, USA). The identity of the *F. alocis* D-62D was confirmed by 16s rRNA gene sequencing (D-62D, accession # GU968904). *F. alocis* strains were grown initially in Robertson's bullock heart medium followed by adaptation to Brain heart infusion broth supplemented with hemin (5 μg/mL), vitamin K (0.5 μg/mL), cysteine (1 μg/mL), and arginine (17.42 μg/mL). *Porphyromonas gingivalis* strains were grown in Brain heart infusion (BHI) broth (Difco) supplemented with hemin (5 μg/mL), vitamin K (0.5 μg/mL), and cysteine (0.1%). Blood agar medium was prepared by the addition of sheep blood (5%) and agar (2%). The bacterial cultures were incubated at 37°C in an anaerobic chamber (Coy Manufacturing) in 10% H_2,10% CO_2, and 80%N_2. Growth rates were determined spectrophotometrically (optical density at 600 nm [OD_{600}]).

2.3 Epithelial cell culture

HeLa cells were grown and maintained at 37°C under 5% CO_2 in Dulbecco's modified Eagle's medium supplemented with 10% fetal bovine serum, penicillin (100 IU/mL), streptomycin (100 IU/mL), and amphotericin B (2.5 mg/mL) (Invitrogen, Carlsbad, CA, USA). Confluent stock cultures were trypsinized, adjusted to approximately 5×10^3 cells/mL, seeded (1 mL per well) into 12-well plates (Nunc, Rochester, NY, USA), and further incubated for 48 h to reach semiconfluency (10^5 cells per well).

2.4 Adherence and standard antibiotic protection assay

Invasion of epithelial cells was quantified using the standard antibiotic protection assay [33]. Briefly, an isolated bacterial colony harvested from solid agar plate was grown to exponential phase in BHI broth. The bacterial cells were then centrifuged, washed three times in PBS, and adjusted to 10^7 CFU/mL of bacteria in DMEM. The epithelial cell monolayer was washed three times with PBS, infected with bacteria at an multiplicity of infection (MOI) of 1:100 (10^5 epithelial cells) and then incubated at 37°C for 30 and 45 min under 5% CO_2. Nonadherent bacteria were removed by washing with PBS while cell surface bound bacteria were killed with metronidazole (200 μg/mL, 60 min). *F. alocis* was sensitive to 100 μg/mL of metronidazole. After removal of the antibiotic, the internalized bacteria were released by osmotic lysis of the epithelial cells in sterile distilled water. Lysates were serially diluted, plated (in duplicate) on BHI agar, and incubated for 6–10 days. The number of bacterial cells recovered was expressed as a percentage of the original inoculum. The number of adherent bacteria was obtained by subtracting the number of intracellular bacteria from the total bacteria obtained in the absence of metronidazole [34]. Coinfection was performed as described previously [2]. *F. alocis* and *P. gingivalis* inocula were prepared by mixing equal volumes (1×10^7 cells/well) of bacterial suspension, which was then incubated

for 5 min in the anaerobic chamber prior to infection. The serially diluted lysate was plated on BHI blood agar and incubated for 6–10 days. The bacterial colonies were phenotypically identified.

2.5 Real-time PCR analysis

Total RNA (1 μg) was reverse transcribed to cDNA using SV total RNA isolation system (Promega, CA) in the presence of random primers (50 ng) according to the manufacturer's recommendations. Real-time PCR was carried out using the Smart cycler II, Cephid. The primers for the real-time analysis (Supporting Information Table 1) were designed using Primer3 software (http://primer3.sourceforge.net/). The amplification efficiency of each primer set was determined empirically by using cDNA template dilutions over four orders of magnitude. The amplification efficiency for each primer set varied between 95.1 and 102.5%, showing that the amplicons were generated with comparable efficiency. The realtime PCR reaction contained 12.5 μL of QuantiTect SYBR Green qPCR master mix (Qiagen), 0.2 μM of each gene-specific primer, and 1 μL of cDNA template. The cycling conditions were 50°C for 2 min, 95°C for 2 min, then 40 cycles of 94°C for 15 s, 58°C for 30 s, and 72°C for 30 s. Distilled water was included as a negative control in each run. All reactions were carried out in triplicate and melting curve analysis indicated that in each reaction a single product was amplified. For all reactions, 16s ribosomal RNA gene (HMPREF 0389_03102) was selected as normalizer. The critical threshold cycle (Ct) for each gene and the relative expression ratio of the selected genes were calculated and analyzed using the relative expression software tool (REST) http://www.gene-quantification.info [35].

2.6 Cell fractionation and SDS-PAGE analysis

Bacterial cells were fractionated as described previously [36]. Briefly, an overnight liquid culture of *F. alocis* was harvested by centrifugation (5000 × *g*, 10 min, 4°C). The supernatant and the pellet were collected separately. To further remove cell debris, the supernatant was again centrifuged at 4000 × *g* for 15 min (4°C), and then concentrated using the Amicon ultrafiltration system (EMD Millipore). The concentrated supernatant was further subjected to ultracentrifugation at 100 000 × *g* for 1 h at 4°C to produce the extracellular fraction. The pellet containing the cells was resuspended in ice-cold PBS. Cells were lysed in a French press (American Instrument company, MD, USA) at 20 000 lb/inch^2. The lysate was cleared of unlysed cells by centrifugation (5000 × *g*, 10 min, 4°C). To separate the membrane fractions from the cytosolic fractions, the lysate was further ultracentrifuged (100 000 × *g*, 1 h, 4°C). The supernatant containing cytosolic fractions was decanted from the pellet that contained the membrane fraction.

SDS-PAGE was used at 4–12% Bis-Tris separating gel in MOPS-SDS running buffer according to the manufacturer's instructions (NuPAGE Novex gels; Invitrogen). Samples were prepared (65% sample, 25% 4× NuPAGE LDS sample buffer, 10% NuPAGE reducing agent), heated at 72°C for 10 min, and then electrophoresed at 200 V for 65 min in the XCell SureLock Mini-Cell System (Invitrogen). The protein bands were visualized with Simply Blue Safe Stain (Invitrogen).

2.7 2D-PAGE analysis

2DE was carried out using the 2D gel strips (7 cm) of p*I* 3–10 in a Protean IEF cell (Bio-Rad, USA) following the method of Poznanovic [37]. Briefly, the protein concentration of the sample was measured using the Bio-Rad spectrophotometer. The protein samples were diluted to a final concentration of 30–50 μg protein and 20 μL of the sample was added to solubilization buffer (7 M urea, 2 M thiourea, 2% w/v CHAPS, 65 mM DTT, bromophenol blue 0.002%, Zwittergent (3–10) 1% w/v). The first-dimension IPG strip was run by adding 125 μL of the diluted sample in the rehydration buffer (730 mg DTT, 70 mg Iodoacetemide) for 8 h at voltage gradients of 3 h at 300 V, 5 h at linear gradients of 300–3500 V, 18 h at 3500 V. After equilibration, the IPG strips were loaded on the gel and electrophoresed at 200 V, 0.3 A for 4–5 h, and then stained with Coomassie Simply Blue strain. 2D gel analysis was performed twice using biological replicates.

2.8 MS and data analysis

An LCQ Deca XP Plus system (www.thermo.com) was used to analyze the extracted peptides from each gel piece [38]. The four part protocol used for the MS and MS/MS analyses, included one full MS analysis (from 450 to 1750 *m/z*) followed by three MS/MS events using data-dependent acquisition, where the most intense ion from a given full MS scan was subjected to collision-induced dissociation, followed by the second and third most intense ions. The nanoflow buffer gradient was extended over 45 min in conjunction with the cycle repeating itself every 2 s, using a 0–60% ACN gradient from buffer B (95% ACN with 0.1% formic acid) developed against buffer A (2% ACN with 0.1% formic acid) at a flow rate of 250–300 nL/min, with a final 5-min 80% bump of buffer B before equilibration. In order to move the 20 μL sample from the autosampler to the nanospray unit, flow stream splitting (1:1000) and an automated valve together with a nanotrap column was used. The spray voltage and current were set at 2.2 kV and 5.0 μA, with a capillary voltage of 25 V in positive ion mode. For peptides, 160°C was used as the spray temperature. Data collection was achieved using the Xcalibur software (Thermo Electron), then screened with Bioworks 3.1. The MASCOT software (www.matrixscience.com) was used for each analysis to produce unfiltered data and out files. Statistical validation of peptide and protein findings was achieved using X TANDEM (www.thegmp.org) and SCAFFOLD meta analysis software (www.proteomesoftware.com). The presence of two different peptides at a probability of at least 95% was required for consideration as being positively identified. General protein database search was conducted using UniprotKb–Protein knowledgebase database (http://www.uniprot.org/uniprot/Filifactoralocis). *F. alocis* ORF database is based on the latest release of the *F. alocis* genome at the NCBI genome project (http://www.ncbi.nlm.nih.gov/nuccore/CP002390.1).

3. Results and discussion

3.1 Several putative virulence factors are modulated in *F. alocis* during invasion of HeLa cells

In a previous report, *F. alocis* D-62D showed an increased invasive capacity of HeLa cells compared to the type strain (*F. alocis* ATCC 35896) [18]. Several putative virulence factors including neutrophil-activating protein A (NAPA) (HMPREF0389_01654) and calcium-

binding acid repeat protein (CBARP) (HMPREF0389_01532) were identified from the proteome of *F. alocis* ATCC 35896 [18]. In addition, an interrogation of the genome of *F. alocis* ATCC 35896 revealed several proteases such as metal-dependent proteases, CaaX proteases, sialoglycoproteases, and calcium-dependent proteases (http://www.ncbi.nlm.nih.gov/genomeprj/46625). Proteases are important virulence factors in oral pathogens including *P. gingivalis* [39, 40]. To determine if the variation in the invasive capacity of epithelial cells by *F. alocis* strains may be correlated with the expression of several of these putative virulence factors, we evaluated their expression during infection of HeLa cells. Infection with a coculture of *P. gingivalis* and the *F. alocis* strains at 30 and 45 min post infection showed an upregulation of several of the putative virulence factors only in *F. alocis* D-62D. Increased expression of the Caax protease (HMPREF0389_00677) at 30 min and ATP-dependent protease La (HMPREF0389_00279) at 45 min were observed for *F. alocis* ATCC 35896. As shown in Fig. 1A, there was an upregulation of the genes encoding the Caax protease (HMPREF0389_00590), Caax protease (HMPREF0389_00677), Xaa-pro-dipeptidase (HMPREF0389_01538), Protease (HMPREF0389_00122), NAPA (HMPREF0389_01654), and CBARP (HMPREF0389_01532) at 30 min post infection of HeLa cells with *F. alocis* D-62D (Fig. 1A). Expressions of these genes, except the Xaa-pro-dipeptidase (HMPREF0389_1538) protease, were not upregulated in HeLa cells infected with *F. alocis* ATCC 35896. At 45-min post infection, the expression level of the Xaa-pro-dipeptidase gene was increased more than threefold while the Protease–00122 *(HMPREF0389_00122)* gene was upregulated more than 4.5-fold. The NAPA and CBARP genes were found to be upregulated 5- and 7.8-folds, respectively (Fig. 1B). Taken together, these results suggest that there is differential expression of several putative virulence genes in *F. alocis* D-62D compared to the type strain *F. alocis ATCC* 35896. The relative significance of these genes in the virulence potential of *F. alocis* is unclear and is under study in the laboratory.

3.2 Proteome variation in *F. alocis* strains

A comparative SDS-PAGE analysis of cell fractions from *F. alocis* ATCC 35896 strain and the D-62D strain showed variation in their protein profile [18]. A random pick of 22 intense protein bands among the various fractions were subjected to MS/MS analysis. As shown in Fig. 2, the identity of these proteins includes several proteins that are known virulence factors in other bacteria [18, 19, 21, 23, 41–51]. To further evaluate other variations that may contribute to the relative pathogenic potential of *F. alocis*, the proteome of *F. alocis* D-62D was compared to the type strain *F. alocis* ATCC 35896. Extracellular and membrane fractions from both these strains were subjected to 2D PAGE analysis (Figs. 3–6). The pattern of spots were reproducible both in technical and biological replicates. The spots were manually excised from the respective gels, in-gel digested with trypsin, and subjected to MS/MS analysis. A total of approximately 1568 peptides were identified that were above the threshold ($p < 0.05$) and had a Mascot score of ≥ 15 with individual ion score of more than 20. A total of 986 nonredundant peptides corresponding to 219 proteins were identified with at least two peptides above the threshold ($p < 0.05$) for each protein. A complete proteome profiling of various fractions of *F. alocis* strains are summarized in Tables 1–4.

In the membrane fraction, there were 50 distinct reproducible spots identified in the *F. alocis* ATCC strain (Fig. 3) as compared to 56 spots in *F. alocis* D-62D strain (Fig. 4). The proteins identified in the membrane fraction are summarized in Tables 1 and 2. Several groups of very intense spots in the range of 30 –60 kDa were observed in *F. alocis* ATCC 35896. While some of these intense spots were noted at the same range in the D-62D strain, there were higher molecular weight protein spots between 260 and 70 kDa that were missing in the ATCC strain (Table 1). Intense protein spots corresponding to copper amine oxidase (HMPREF0389_00784), leukotoxin ATP-binding translocation protein (HMPREF0389_1580) were present in both the strains, however, protein spots corresponding to CBARP (HMPREF0389_1532), layer Y-domain protein (HMPREF0389_1139), peptidoglycan biosynthesis transpeptidase (HMPREF0389_00555), and fibronectin-binding protein (HMPREF0389_00575) were present only in the *F. alocis* D-62D strain (Table 2). All these spots corresponded to high molecular weight proteins ranging from 205 to 68 kDa. Several hypothetical proteins, common to both *F. alocis* strains were identified in the membrane fraction. Based on the domain prediction, proteins corresponding to protein secretory pathways such as hypothetical protein (HMPREF0389_1740)–(Sec pathway) and Type IV pilus assembly protein (HMPREF0389_00426)–(Type II secretion system) were noted in the ATCC strain. The protein export membrane protein (HMPREF0389_1478) predicted to be involved in the Sec pathway was identified in the *F. alocis* D-62D strain. While the membrane fraction of *F. alocis* ATCC strain showed only the Caax amino protease (HMPREF0389_00590), the more virulent *F. alocis* D-62D strain had nine proteins belonging to the protease/peptidase family: peptidoglycan biosynthesis transpeptidase, peptidase M23/M37, oligo endopeptidase F, amino acyl histidine dipeptidase, Caax amino protease, Xaa pro-dipeptidase (HMPREF0389_1538), signal peptidase, ATP-dependent RIP metalloprotease, O-sialoglycoprotein endopeptidase. It is noteworthy that the Xaa pro dipeptidase was shown to be highly upregulated during coculture of *F. alocis* with *P. gingivalis* [18]. Other high molecular weight proteins, identified in *F. alocis* D-62D include acetyl ornithine transaminase (HMPREF0389_1570), membrane protein (HMPREF0389_00019), pyridoxine biosynthesis protein (HMPREF0389_00858), NG, NG dimethyl arginine, dimethyl amino hydrolase (HMPREF0389_1354), toxin antitoxin component ribbon helix–helix fold protein (HMPREF0389_00243), and hypothetical protein (HMPREF0389_01030). Homologs of several proteins involved in cell wall biosynthesis in *S. mutans* [21] (peptidoglycan biosynthesis transpeptidase (HMPREF0389_00555)), antibiotic resistance in *F. nucleatum* [23] (tetracycline-resistant protein (HMPREF0389_01071)), and virulence in *P. gingivalis* [52] (trigger factor (HMPREF0389_1646)), and DNA-binding response regulator protein (HMPREF0389_01693 with respective domain) were also observed in the membrane fraction of both strains.

In the extracellular fraction, a total of 54 and 57 nonredundant reproducible proteins were identified in *F. alocis* ATCC 35896 and D-62D, respectively (Figs. 5 and 6, Tables 3 and 4). Intense protein spots were found between 30 and 75 kDa in the ATCC 35896 strain. Though similar proteins were identified in the two strains, proteins such as cell wall serine protease (HMPREF0389_01110), conserved hypothetical protein (HMPREF0389_01728), hypothetical protein (HMPREF0389_01692), protease (HMPREF0389_00122), ATP-

dependent protease La (HMPREF0389_00279), and leucotoxin translocation ATP-binding protein (HMPREF0389_01580) were identified only in the extracellular fraction of *F. alocis* D-62D, the more virulent strain. Leucotox in is known as a membrane-active toxin that specially targets human polymorphonuclear leucocytes and monocytes [53]. While it can remain associated with the bacterial cell surface, its secretion is mediated by a Type I secretion system in Gram-negative bacteria [54]. It is unknown if there is a defect in the secretion system of *F. alocis* ATCC 35896 or other factors may alter the secretion of the leucotoxin. In *A. actinomycetemcomitans*, lipopolysaccharide can mediate leukotoxin secretion [55]. Proteins such as fibronectin-binding protein [56] and S layer protein [57] that are secreted by Type-1 secretion system in other bacteria were found in the extracellular fraction of both the *F. alocis* strains likely, suggesting the presence of a Type 1 secretory system. A secretion mechanism and the impact of leucotoxin secretion in *F. alocis* pathogenesis are under study in the laboratory. An intense protein spot of molecular weight 34.9 kDa corresponding to the conserved hypothetical protein (HMPREF0389_01401) was noted exclusively in *F. alocis* D-62D. (Table 4). Even though the lower molecular weight proteins between 10 and 25 kDa were noted in *F. alocis* ATCC 35896, conserved hypothetical proteins (HMPREF0389_00741), (HMPREF0389_00321), and (HMPREF0389_01744) were found only in *F. alcois* D-62D. These three conserved hypothetical proteins showed no specific conserved domains. It was also interesting to note that six hypothetical proteins including HMPREF0389_01693, HMPREF0389_01750, HMPREF0389_00607, HMPREF0389_01489, HMPREF0389_01177, and HMPREF0389_01239 were unique to the *F. alocis* ATCC 35896. Among them, three were found to be involved with the regulation of cell function.

3.3 Amino acid metabolism

Consistent with its assacharolytic properties, several proteins that play an important role in this process were identified in both membrane and extracellular fractions of *F. alcois.* Certain oral bacteria such as *F. nucleatum* lack essential amino acid synthetic pathways and rely on the ability to import and degrade di- and oligopeptides [58]. With the occurrence of a wide range of such dipeptidases, metalloproteases and O-sialoglycoproteases (refer Table 5), *F. alocis*, could also lack some inherent amino acid synthesis pathways but could alternate through degradation of proteins with the help of such proteases and peptidase. It is important to note that protein spots corresponding to ornithine transaminase (HMPREF0389_01570), acetyl glutamate kinase (HMPREF0389_01569), glutamate racemase (HMPREF0389_00100), and amidotransferase (HMPREF0389_00478) involved in ornithine biosynthesis were identified. These proteins were found both in the membrane and the extracellular fraction of the D-62D strain. Proteins involved in ornithine catabolism and urea breakdown, namely arginine deiminase (HMPREF0389_01584), were also noted. Taken together, it is likely that *F. alocis* could have a well-developed nitrogen assimilatory pathway that is needed for alternative mode of amino acid synthesis [59].

Certain proteins such as oxy acyl carrier protein (HMPREF0389_ 01112) involved in fatty acid metabolism and not usually identified among the oral biofilm forming pathogens, was identified in *F. alocis* [60]. Strain-specific proteins such as fibronectin-binding protein

(HMPREF0389_00575) and dipicolinate reductase (HMPREF0389_01077) involved in amino acid metabolism and virulence [61] were noted in the D-62D strain of *F. alocis*.

3.4 Proteases

In bacteria, proteolysis plays an important role in many biological processes such as posttranslational regulation of gene expression, processing, and maturation of various surface-associated proteins in Gram-positive bacteria [62, 63]. Proteases have been one of the virulence attributes among many oral pathogens [7,39,64]. Expression of various surface proteins depends on proteolysis that could strongly influence both the level of activity of proteases and their cellular localization [44]. In our study, strain variations were noted among the proteases in both membrane and the extracellular fraction of *F. alocis* strains. Among the membrane-bound proteases of *F. alocis,* Caax protease (HMPREF0389_00590) has been identified in both the strains of *F. alocis.* The Caax amino proteases could be involved in the protein and/or peptide modification and secretion [50]. Caax amino-terminal proteases of *S. gordonii* have been demonstrated to play a role in transport of proteins and protect the bacteria against bacteriocins, other than their metalloprotease activity [65]. The Xaa-pro-dipeptidase (HMPREF0389_01538), O-sialoendopeptidase (HMPREF0389_01445), peptidase M23/37 (HMPREF0389_00239), and oligo endopeptidase F (HMPREF0389_00926) were also identified only in the membrane fraction of the *F. alocis* D-62D strain. However, protease (HMPREF0389_00122) was identified only in the extracellular fraction of D-62D strain. Based on motif search and domain prediction studies, this protease is predicted to possess a collagen peptidase function. The role of such protease could be important in *F. alocis* pathogenesis as it has the potential to damage the connective tissue of the gingiva. Several oral pathogens are known to produce or induce host-derived collagenases that are implicated in tissue destruction in periodontal diseases [66–68]. The role of several of the proteases in *F. alocis* pathogenesis is under further investigation.

3.5 Secretory system

In general, certain oral pathogens such as *Fusobacteria* are known to secrete few proteins and lack the genes encoding the components of the major secretory systems [58]. However, in *F. alocis* a conserved hypothetical protein (HMPREF0389_00315)—a secretory system-II pilus domain containing protein was identified in the ATCC strain. Proteins involved in type-II secretory pathway, namely, Type IV pilus assembly protein (HMPREF0389_00426) and trigger factor (HMPREF0389_01646), were also identified in the membrane fraction of the *F. alocis* ATCC 35896. The membrane fraction of the *F. alcois* D-62D showed proteins involved in the Sec pathway such as, fimbrial assembly protein (HMPREF0389_00415) and protein export membrane protein (HMPREF0389_01478) (containing SecD and SecF domains). A total of seven proteins predicted to be involved in protein transport were noted in the D-62D strain. The relative abundance of these proteins was less in the type strain compared to the *F. alocis* D-62D (Table 6). Hence, it is likely that *F. alocis* has a well-developed type-II and Sec-dependent protein transport pathway that could vary based on the relative virulence of the pathogen and/or its interaction with other organisms.

3.6 Virulence

Several proteins known to be involved in virulence in other bacteria were observed in both the membrane and extracellular fractions of *F. alocis* D-62D. CBARP (HMPREF0389_01532), leucotoxin translocation ATP-binding protein (HMPREF0389_01580), fibronectin-binding protein (HMPREF0389_00575), Type IV pilus assembly protein (HMPREF0389_00416), fimbrial assembly protein (HMPREF0389_00415), Hemolysin III type calcium-binding protein (HMPREF0389_01477), toxin–antitoxin component protein (HMPREF0389_00243), and NAPA (HMPREF0389_01654) were observed in the membrane fraction. There was also expression of CBARP, leucotoxin translocation ATP-binding protein, fibronectin-binding proteins, and NAPA in the extracellular fraction, in addition to the TetR family transcription regulator (HMPREF0389_00975) and tetracycline-resistant protein (HMPREF0389_01071). Similar to *T. denticola*, *Clostridium botulinum*, and *P. gingivalis*, there was expression of S-layer protein (HMPREF0389_01139) that was only observed in the membrane fraction of *F. alocis* D-62D [58]. Several glycolytic enzymes such as phosphoglycerate mutase (HMPREF0389_1582) and glyceraldehyde-3-phosphate dehydrogenase (HMPREF0389_00567) that are basically involved in energy metabolism were both identified in the extracellular fraction of *F. alocis*. Such proteins could have a moonlighting function as plasminogen-binding protein and adhesins for fibronectin and plasminnogens, respectively [69]. Protein moonlighting contributes to bacterial virulence in a number of important human pathogens [70].

3.7 In silico analysis of the membrane proteins

Surface proteins are important factors in the interaction of pathogenic bacteria with their environment and host [71]. A comparative bioinformatic analysis of the membrane proteins between the D-62D and the type strains of *F. alocis* revealed more cell wall anchor domain containing proteins (Table 7; Supporting Information Table 2). One subgroup of these proteins is the sortase-dependent proteins that have a C terminal *LP×TG* motif [72]. There are various groups of sortase enzymes with specific motifs, namely, a sortase B motif of *NP(Q/K)(T/S)(N/G/S)(D/A)*, Sortase D motif of *LP×TA*, and other atypical sortase anchor motifs resembling the *LP×TG* motifs with minor variations [72]. Our study found more proteins with these motifs in the *F. alocis* D-62D strain in contrast to the type strain. Using the annotated genome sequence of *F. alocis*, we observed that more than 25% of the membrane proteins of the D-62D strain showed N-terminal signal sequences. The majority of these proteins also carried a signal peptidase I cleavage site that could have secretory/membrane targeting functions. Approximately 25% of the total membrane proteins were found to possess transmembrane helix domain and hence may be involved in protein transport [73]. Several proteins with a common motif known to play a role in membrane anchorage were observed in both *F. alocis* strains. More of these proteins were unique to *F. alocis* D-62D. Proteins can also be anchored to the envelope by LysM domains that bind to the peptidoglycan in the bacterial cell wall [74]. There are four LysM domain proteins as compared to two in the type strain. Kleerebezem and co-workers [75] identified a novel C terminal W×L domain that they proposed could be a binding domain for the cell envelope. In this study, six proteins containing this domain were identified in the D-62D strain of *F.*

alocis. It is noteworthy that of the 56 membrane proteins identified in *F. alocis* D-62D, 20 contain the peptidoglycan-binding domain that amounts to 36% of the total membrane proteins identified. Upon sequence alignment of the membrane proteins of the D-62D strain, it was evident that 25 proteins contain a C-terminal glycine rich domain with a concensus GxxGxGxGx motif (Supporting Information Fig. 1). Such C-terminal glycine rich domain was not identified in the type strain membrane proteins. Such glycine rich motifs are crucial for RNA binding [76]. Hence, from this in silico study of membrane proteins it could be inferred that *F. aloics* might have a well-developed protein secretory and transport system that could play a role in its pathogenic potential. The metabolic pathway analysis revealed no significant difference between the two strains.

4 Concluding remarks

This study identified several membrane-associated and extracellular proteins from *F. alocis.* Although the number of proteins identified was lower than the expected, bacteria are known to modulate specific genes in response to their environment [77]. In practice, many low abundance proteins, particularly intrinsic cytoplasmic membrane proteins although representing 15–30% of the proteome of a bacterium, are either not detected or represent less than 1% of the proteins displayed on the 2D gel [77]. Proteins including several proteases, NAPA, and CBARP were identified in *F. alocis*. The genes encoding these proteins were upregulated during infection of epithelial cells. A comparative in silico analysis among the D-62D and type strains of *F. alocis* revealed more cell wall anchoring proteins in the D-62D strain, suggesting the role of such proteins in protein secretion and virulence. Their expression was enhanced by coinfection with *P. gingivalis.* The variation in the pathogenic potential of the *F. alocis* strains may be related to the differential expression of several putative virulence factors. Future work is needed to understand the regulation of these genes in addition to their relative significance in *F. alocis*. A genome-wide association study of *F. alocis* strains is in progress to evaluate variations at the genome level.

Acknowledgments

This work was supported by Loma Linda University and Public Health Grants DE022724, DE13664, and DE019730 from NIDCR (to H.M.F.). We thank Floyd E. Dewhirst for the gift of the F. alocis D-62D isolate.

References

1. Rudney JD, Chen R, Sedgewick GJ. Intracellular *Actinobacillus actinomycetemcomitans* and *Porphyromonas gingivalis* in buccal epithelial cells collected from human subjects. Infect Immun. 2001; 69:2700–2707. [PubMed: 11254637]
2. Saito A, Inagaki S, Kimizuka R, Okuda K, et al. *Fusobacterium nucleatum* enhances invasion of human gingival epithelial and aortic endothelial cells by *Porphyromonas gingivalis*. FEMS Immunol Med Microbiol. 2008; 54:349–355. [PubMed: 19049647]
3. Saito A, Inagaki S, Ishihara K. Differential ability of periodontopathic bacteria to modulate invasion of human gingival epithelial cells by *Porphyromonas gingivalis*. Microb Pathog. 2009; 47:329–333. [PubMed: 19818393]
4. Amano A. Disruption of epithelial barrier and impairment of cellular function by *Porphyromonas gingivalis*. Front Biosci. 2007; 12:3965–3974. [PubMed: 17485350]
5. Dewhirst FE, Chen T, Izard J, Paster BJ, et al. The human oral microbiome. J Bacteriol. 2010; 192:5002–5017. [PubMed: 20656903]

6. Gross EL, Leys EJ, Gasparovich SR, Firestone ND, et al. Bacterial 16S sequence analysis of severe caries in young permanent teeth. J Clin Microbiol. 2010; 48:4121–4128. [PubMed: 20826648]
7. Paster BJ, Boches SK, Galvin JL, Ericson RE, et al. Bacterial diversity in human subgingival plaque. J Bacteriol. 2001; 183:3770–3783. [PubMed: 11371542]
8. Ahn J, Yang L, Paster BJ, Ganly I, et al. Oral microbiome profiles: 16S rRNA pyrosequencing and microarray assay comparison. PLoS One. 2011; 6:e22788. [PubMed: 21829515]
9. Griffen AL, Beall CJ, Campbell JH, Firestone ND, et al. Distinct and complex bacterial profiles in human periodontitis and health revealed by 16S pyrosequencing. ISME J. 2012; 6:1176–1185. [PubMed: 22170420]
10. D'Elios MM, Amedei A, Cappon A, Del PG, de BM. The neutrophil-activating protein of Helicobacter pylori (HP-NAP) as an immune modulating agent. FEMS Immunol Med Microbiol. 2007; 50:157–164. [PubMed: 17521355]
11. Feuille F, Ebersole JL, Kesavalu L, Stepfen MJ, Holt SC. Mixed infection with *Porphyromonas gingivalis* and *Fusobacterium nucleatum* in a murine lesion model: potential synergistic effects on virulence. Infect Immun. 1996; 64:2094–2100. [PubMed: 8675312]
12. Ryder MI. Comparison of neutrophil functions in aggressive and chronic periodontitis. Periodontology 2000. 2010; 53:124–137. [PubMed: 20403109]
13. Kumar PS, Griffen AL, Barton JA, Paster BJ, et al. New bacterial species associated with chronic periodontitis. J Dent Res. 2003; 82:338–344. [PubMed: 12709498]
14. Kumar PS, Leys EJ, Bryk JM, Martinez FJ, et al. Changes in periodontal health status are associated with bacterial community shifts as assessed by quantitative 16S cloning and sequencing. J Clin Microbiol. 2006; 44:3665–3673. [PubMed: 17021095]
15. Wade WG. Has the use of molecular methods for the characterization of the human oral microbiome changed our understanding of the role of bacteria in the pathogenesis of periodontal disease? J Clin Periodontol. 2011; 38:7–16. [PubMed: 21323699]
16. Cato EP, Moore LVH, Moore WEC. *Fusobacterium alocis* sp. nov. and *Fusobacterium sulci* sp. nov. from the human gingival sulcus. Int J Syst Bacteriol. 1985:475–477.
17. Jalava J, Eerola E. Phylogenetic analysis of *Fusobacterium alocis* and *Fusobacterium sulci* based on 16S rRNA gene sequences: proposal of *Filifactor alocis* (Cato, Moore and Moore) comb. nov. and Eubacterium sulci (Cato, Moore and Moore) comb. nov. Int J Syst Bacteriol. 1999; 49:1375–1379. [PubMed: 10555315]
18. Aruni AW, Roy F, Fletcher HM. *Filifactor alocis* has virulence attributes that can enhance its persistence under oxidative stress conditions and mediate invasion of epithelial cells by *Porphyromonas gingivalis*. Infect Immun. 2011; 79:3872–3886. [PubMed: 21825062]
19. Mofatt CE, Whitmore SE, Griffen AL, Leys EJ, Lamont RJ. *Filifactor alocis* interactions with gingival epithelial cells. Mol Oral Microbiol. 2011; 26:365–373. [PubMed: 22053964]
20. Ramsey MM, Rumbaugh KP, Whiteley M. Metabolite cross-feeding enhances virulence in a model polymicrobial infection. PLoS Pathog. 2011; 7:e1002012. [PubMed: 21483753]
21. Guo LH, Wang HL, Liu XD, Duan J. Identification of protein differences between two clinical isolates of *Streptococcus mutans* by proteomic analysis. Oral Microbiol Immunol. 2008; 23:105–111. [PubMed: 18279177]
22. Wilkins JC, Homer KA, Beighton D. Altered protein expression of *Streptococcus oralis* cultured at low pH revealed by two-dimensional gel electrophoresis. Appl Environ Microbiol. 2001; 67:3396–3405. [PubMed: 11472910]
23. Al-Haroni M, Skaug N, Bakken V, Cash P. Proteomic analysis of ampicillin-resistant oral *Fusobacterium nucleatum*. Oral Microbiol Immunol. 2008; 23:36–42. [PubMed: 18173796]
24. Lamont RJ, Meila M, Xia Q, Hackett M. Mass spectrometry-based proteomics and its application to studies of *Porphyromonas gingivalis* invasion and pathogenicity. Infect Disord Drug Targets. 2006; 6:311–325. [PubMed: 16918489]
25. Tamura K, Dudley J, Nei M, Kumar S. MEGA4: molecular evolutionary genetics analysis (MEGA) software version 4.0. Mol Biol Evol. 2007; 24:1596–1599. [PubMed: 17488738]
26. Johnson LS, Eddy SR, Portugaly E. Hidden Markov model speed heuristic and iterative HMM search procedure. BMC Bioinform. 2010; 11:431.

27. Kanehisa M, Goto S, Furumichi M, Tanabe M, Hirakawa M. KEGG for representation and analysis of molecular networks involving diseases and drugs. Nucleic Acids Res. 2010; 38:D355–D360. [PubMed: 19880382]
28. Bendtsen JD, Nielsen H, von HG, Brunak S. Improved prediction of signal peptides: SignalP 3.0. J Mol Biol. 2004; 340:783–795. [PubMed: 15223320]
29. Krogh A, Larsson B, von HG, Sonnhammer EL. Predicting transmembrane protein topology with a hidden Markov model: application to complete genomes. J Mol Biol. 2001; 305:567–580. [PubMed: 11152613]
30. Punta M, Coggill PC, Eberhardt RY, Mistry J, et al. The Pfam protein families database. Nucleic Acids Res. 2012; 40:D290–D301. [PubMed: 22127870]
31. Sutcliffe IC, Harrington DJ. Pattern searches for the identification of putative lipoprotein genes in Gram-positive bacterial genomes. Microbiology. 2002; 148:2065–2077. [PubMed: 12101295]
32. Boekhorst J, de Been MW, Kleerebezem M, Siezen RJ. Genome-wide detection and analysis of cell wall-bound proteins with LP×TG-like sorting motifs. J Bacteriol. 2005; 187:4928–4934. [PubMed: 15995208]
33. Yilmaz O, Young PA, Lamont RJ, Kenny GE. Gingival epithelial cell signalling and cytoskeletal responses to *Porphyromonas gingivalis* invasion. Microbiology. 2003; 149:2417–2426. [PubMed: 12949167]
34. Castaneda-Roldan EI, velino-Flores F, Dall'Agnol M, Freer E, et al. Adherence of Brucella to human epithelial cells and macrophages is mediated by sialic acid residues. Cell Microbiol. 2004; 6:435–445. [PubMed: 15056214]
35. Pfaffl MW, Horgan GW, Dempfle L. Relative expression software tool (REST) for group-wise comparison and statistical analysis of relative expression results in real-time PCR. Nucleic Acids Res. 2002; 30:e36. [PubMed: 11972351]
36. Fulkerson JF Jr, Mobley HL. Membrane topology of the NixA nickel transporter of *Helicobacter pylori*: two nickel transport-specific motifs within transmembrane helices II and III. J Bacteriol. 2000; 182:1722–1730. [PubMed: 10692379]
37. Poznanovic S, Schwall G, Zengerling H, Cahill MA. Isoelectric focusing in serial immobilized pH gradient gels to improve protein separation in proteomic analysis. Electrophoresis. 2005; 26:3185–3190. [PubMed: 16041705]
38. Henry LG, Sandberg L, Zhang K, Fletcher HM. DNA repair of 8-oxo-7,8-dihydroguanine lesions in *Porphyromonas gingivalis*. J Bacteriol. 2008; 190:7985–7993. [PubMed: 18849425]
39. Lamont RJ, Jenkinson HF. Life below the gum line: pathogenic mechanisms of *Porphyromonas gingivalis*. Microbiol Mol Biol Rev. 1998; 62:1244–1263. [PubMed: 9841671]
40. Potempa J, Mikolajczyk-Pawlinska J, Brassell D, Nelson D, et al. Comparative properties of two cysteine proteinases (gingipains R), the products of two related but individual genes of *Porphyromonas gingivalis*. J Biol Chem. 1998; 273:21648–21657. [PubMed: 9705298]
41. Abdullah KM, Lo RY, Mellors A. Cloning, nucleotide sequence, and expression of the *Pasteurella haemolytica* A1 glycoprotease gene. J Bacteriol. 1991; 173:5597–5603. [PubMed: 1885539]
42. Aruni W, Vanterpool E, Osbourne D, Roy F, et al. Sialidase and sialoglycoproteases can modulate virulence in *Porphyromonas gingivalis*. Infect Immun. 2011; 79:2779–2791. [PubMed: 21502589]
43. Bethe G, Nau R, Wellmer A, Hakenbeck R, et al. The cell wall-associated serine protease PrtA: a highly conserved virulence factor of *Streptococcus pneumoniae*. FEMS Microbiol Lett. 2001; 205:99–104. [PubMed: 11728722]
44. Biswas S, Biswas I. Role of HtrA in surface protein expression and biofilm formation by *Streptococcus mutans*. Infect Immun. 2005; 73:6923–6934. [PubMed: 16177372]
45. Dramsi S, Magnet S, Davison S, Arthur M. Covalent attachment of proteins to peptidoglycan. FEMS Microbiol Rev. 2008; 32:307–320. [PubMed: 18266854]
46. Gazi MI, Cox SW, Clark DT, Eley BM. Comparison of host tissue and bacterial dipeptidyl peptidases in human gingival crevicular fluid by analytical isoelectric focusing. Arch Oral Biol. 1995; 40:731–736. [PubMed: 7487574]
47. Goldstein JM, Kordula T, Moon JL, Mayo JA, Travis J. Characterization of an extracellular dipeptidase from *Streptococcus gordonii* FSS2. Infect Immun. 2005; 73:1256–1259. [PubMed: 15664976]

48. Leiting B, Pryor KD, Wu JK, Marsilio F, et al. Catalytic properties and inhibition of proline-specific dipeptidyl peptidases II, IV and VII. Biochem J. 2003; 371:525–532. [PubMed: 12529175]
49. Nepomuceno RS, Tavares MB, Lemos JA, Griswold AR, et al. The oligopeptide (opp) gene cluster of *Streptococcus mutans*: identification, prevalence, and characterization. Oral Microbiol Immunol. 2007; 22:277–284. [PubMed: 17600541]
50. Pei J, Grishin NV. Type II CAAX prenyl endopeptidases belong to a novel superfamily of putative membrane-bound metalloproteases. Trends Biochem Sci. 2001; 26:275–277. [PubMed: 11343912]
51. Reynaud af GA, Culak R, Molenaar L, Chattaway M, et al. Comparative analysis of virulence determinants and mass spectral profiles of Finnish and Lithuanian endodontic *Enterococcus faecalis* isolates. Oral Microbiol Immunol. 2007; 22:87–94. [PubMed: 17311631]
52. Yoshimura M, Ohara N, Kondo Y, Shoji M, et al. Proteome analysis of *Porphyromonas gingivalis* cells placed in a subcutaneous chamber of mice. Oral Microbiol Immunol. 2008; 23:413–418. [PubMed: 18793365]
53. Johansson A. *Aggregatibacter actinomycetemcomitans* leukotoxin: a powerful tool with capacity to cause imbalance in the host inflammatory response. Toxins (Basel). 2011; 3:242–259. [PubMed: 22069708]
54. Kachlany SC. *Aggregatibacter actinomycetemcomitans* leukotoxin: from threat to therapy. J Dent Res. 2010; 89:561–570. [PubMed: 20200418]
55. Tang G, Kawai T, Komatsuzawa H, Mintz KP. Lipopolysaccharides mediate leukotoxin secretion in *Aggregatibacter actinomycetemcomitans*. Mol Oral Microbiol. 2012; 27:70–82. [PubMed: 22394466]
56. Lannergard J, Flock M, Johansson S, Flock JI, Guss B. Studies of fibronectin-binding proteins of *Streptococcus equi*. Infect Immun. 2005; 73:7243–7251. [PubMed: 16239519]
57. Toporowski MC, Nomellini JF, Awram P, Smit J. Two outer membrane proteins are required for maximal type I secretion of the Caulobacter crescentus S-layer protein. J Bacteriol. 2004; 186:8000–8009. [PubMed: 15547272]
58. Kapatral V, Anderson I, Ivanova N, Reznik G, et al. Genome sequence and analysis of the oral bacterium *Fusobacterium nucleatum* strain ATCC 25586. J Bacteriol. 2002; 184:2005–2018. [PubMed: 11889109]
59. Doroshchuk NA, Gel'fand MS, Rodionov DA. Regulation of nitrogen metabolism in gram-positive bacteria. Mol Biol (Mosk). 2006; 40:919–926. [PubMed: 17086994]
60. Rathsam C, Eaton RE, Simpson CL, Browne GV, et al. Two-dimensional fluorescence difference gel electrophoretic analysis of *Streptococcus mutans* biofilms. J Proteome Res. 2005; 4:2161–2173. [PubMed: 16335963]
61. Berges DA, DeWolf WE Jr, Dunn GL, Newman DJ, et al. Studies on the active site of succinyl-CoA:tetrahydrodipicolinate N-succinyltransferase. Characterization using analogs of tetrahydrodipicolinate. J Biol Chem. 1986; 261:6160–6167. [PubMed: 3700390]
62. Gottesman S, Wickner S, Maurizi MR. Protein quality control: triage by chaperones and proteases. Genes Dev. 1997; 11:815–823. [PubMed: 9106654]
63. Laskowska E, Kuczynska-Wisnik D, Skorko-Glonek J, Taylor A. Degradation by proteases Lon, Clp and HtrA, of *Escherichia coli* proteins aggregated *in vivo* by heat shock; HtrA protease action *in vivo* and *in vitro*. Mol Microbiol. 1996; 22:555–571. [PubMed: 8939438]
64. Curtis MA, duse-Opoku J, Rangarajan M. Cysteine proteases of *Porphyromonas gingivalis*. Crit Rev Oral Biol Med. 2001; 12:192–216. [PubMed: 11497373]
65. Zhang Y, Whiteley M, Kreth J, Lei Y, et al. The two-component system BfrAB regulates expression of ABC transporters in *Streptococcus gordonii* and *Streptococcus sanguinis*. Microbiology. 2009; 155:165–173. [PubMed: 19118357]
66. Holt SC, Kesavalu L, Walker S, Genco CA. Virulence factors of *Porphyromonas gingivalis*. Periodontology. 2000; 20:168–238.
67. Robertson PB, Cobb CM, Taylor RE, Fullmer HM. Activation of latent collagenase by microbial plaque. J Periodontal Res. 1974; 9:81–83. [PubMed: 4368370]

68. Robertson PB, Lantz M, Marucha PT, Kornman KS, et al. Collagenolytic activity associated with Bacteroides species and *Actinobacillus actinomycetemcomitans*. J Periodontal Res. 1982; 17:275–283. [PubMed: 6125580]
69. Henderson B, Nair S, Pallas J, Williams MA. Fibronectin: a multidomain host adhesin targeted by bacterial fibronectin-binding proteins. FEMS Microbiol Rev. 2011; 35:147–200. [PubMed: 20695902]
70. Henderson B, Martin A. Bacterial virulence in the moonlight: multitasking bacterial moonlighting proteins are virulence determinants in infectious disease. Infect Immun. 2011; 79:3476–3491. [PubMed: 21646455]
71. van Pijkeren JP, Canchaya C, Ryan KA, Li Y, et al. Comparative and functional analysis of sortase-dependent proteins in the predicted secretome of *Lactobacillus salivarius* UCC118. Appl Environ Microbiol. 2006; 72:4143–4153. [PubMed: 16751526]
72. Spirig T, Weiner EM, Clubb RT. Sortase enzymes in Gram-positive bacteria. Mol Microbiol. 2011; 82:1044–1059. [PubMed: 22026821]
73. Palmer T, Berks BC. Moving folded proteins across the bacterial cell membrane. Microbiology. 2003; 149:547–556. [PubMed: 12634324]
74. Steen A, Buist G, Leenhouts KJ, El KM, et al. Cell wall attachment of a widely distributed peptidoglycan binding domain is hindered by cell wall constituents. J Biol Chem. 2003; 278:23874–23881. [PubMed: 12684515]
75. Kleerebezem M, Boekhorst J, van KR, Molenaar D, et al. Complete genome sequence of *Lactobacillus plantarum* WCFS1. Proc Natl Acad Sci USA. 2003; 100:1990–1995. [PubMed: 12566566]
76. Fierro-Monti I, Mathews MB. Proteins binding to duplexed RNA: one motif, multiple functions. Trends Biochem Sci. 2000; 25:241–246. [PubMed: 10782096]
77. Len AC, Cordwell SJ, Harty DW, Jacques NA. Cellular and extracellular proteome analysis of *Streptococcus mutans* grown in a chemostat. Proteomics. 2003; 3:627–646. [PubMed: 12748943]

Abbreviations

BHI	Brain heart infusion
NAPA	neutrophil-activating protein A

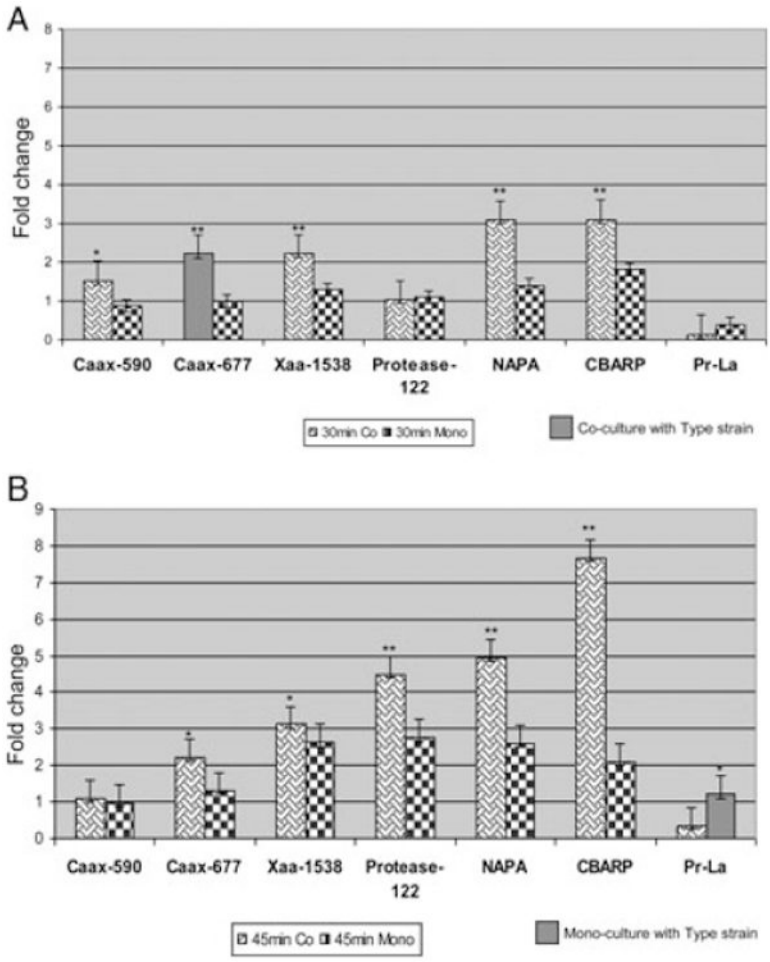

Figure 1.

Quantitative PCR analysis of several putative virulence genes in *F alocis.* (A) 30-min mono- and coculture. (B) 45-min mono- and coculture. Hela cells were infected with *F. alocis* ATCC 35896 and D-62D strains [(MOI of 1:100(105 epithelial cells)] in mono or coculture with *Porphyromonas gingivalis* W83 as previously reported [18]. RNA was isolated at 30- and 45-min post infection using the SV total RNA isolation system (Promega). cDNA was made using the Transcriptor High Fidelity cDNA synthesis kit (Roche). Real-time PCR was performed using the Smart cycler (Cepheid) with gene-specific oligonucleotides. Caax-590 (HMPREF0389_00590); Caax-677 (HMPREF0389_00677); Xaa-1538, Xaa pro dipeptidase (HMPREF0389_01538); NAPA (neutrophil-acitivating factor protein A) (HMPREF0389_01654); Protease-00122 (HMPREF0389_00122); CBARP (calcium-binding acid repeat proteins) (HMPREF0389_01532); Protease La (Pr-La) (HMPREF0389_00279). Fold change was calculated using the formula. Fold change = 2 – ΔΔCt, where ΔΔCt = ΔCt of the sample –ΔCt of reference.
(**$p < 0.01$; *$p < 0.05$).

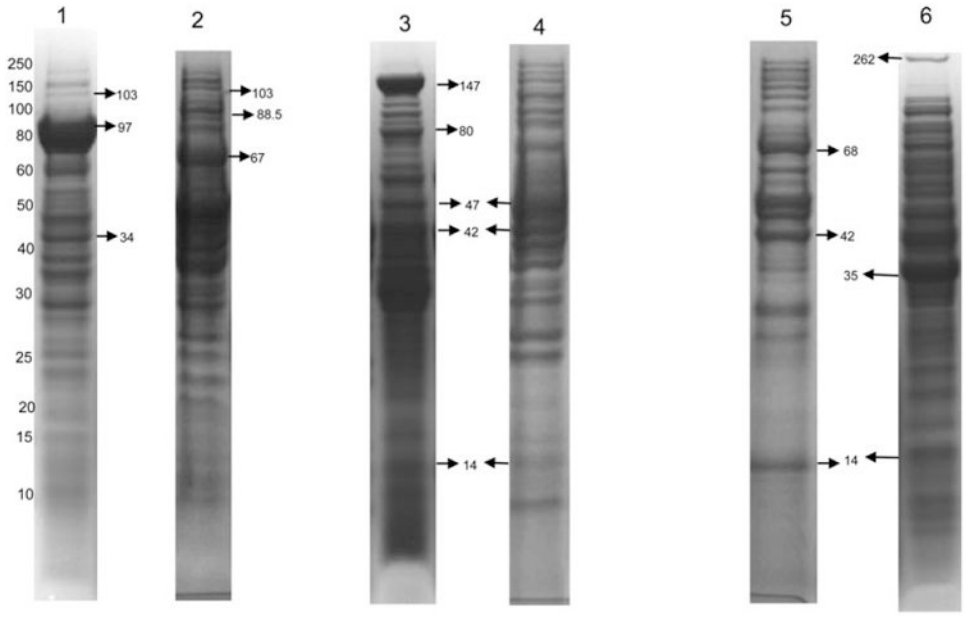

Figure 2.

PAGE of the *F. alocis* protein fractions from the type strain and D-62D. All the lanes show protein bands and their corresponding molecular masses (kDa). Each lane was loaded with 35 μg of protein. The prominent protein bands (shown by arrow) were excised and analyzed by MS. Lane 1: *F. alocis ATCC* 35896—extra cellular fraction. 103 kDa: calcium-binding acid repeat protein (HMPREF0389_01448); 97 kDa: conserved hypothetical protein (HMPREF0389_01431); 34 kDa: cobalt import ATP-binding protein (HMPREF0389_00901). Lane 2: *F alocis* D-62D-extra cellular fraction. 103 kDa: calcium-binding acid repeat protein (HMPREF0389_01448); 88.5 kDa: protease (HMPREF0389_00122); 67 kDa: S layer Y domain containing protein (HMPREF0389_00223). Lane 3: *F alocis ATCC* 35896—membrane fraction. 147 kDa: S layer Y domain containing protein (HMPREF0389_01139); 80 kDa: membrane protein (HMPREF0389_000638); 47 kDa: Caax protease (HMPREF0389_00590); 42 kDa: Xaa pro-dipeptidase (HMPREF0389_01538); 14 kDa: neutrophil-activating protein A (HMPREF0389_01654). Lane 4: *Falocis* D-62D— membrane fraction; 47 kDa: Caax protease (HMPREF0389_00590); 42 kDa: Xaa pro-dipeptidase (HMPREF0389_01538); 14 kDa: neutrophil-activating protein A (HMPREF0389_01654). Lane 5: *F alocis ATCC* 35896—cytosolic fraction. 68 kDa: fibronectin-binding protein (HMPREF 0389_00575); 42 kDa: Xaa pro-dipeptidase (HMPREF0389_01538); 14 kDa: neutrophil-activating protein A (HMPREF0389_01654). Lane 6: *F. alocis* D-62D—cytosolic fraction. 262 kDa: cell wall associated serine proteinase (HMPREF0389_01110); 35 kDa: electron transfer flavo-protein alpha (HMPREF0389_00742); 14 kDa: neutrophil-activating protein A (HMPREF0389_01654).

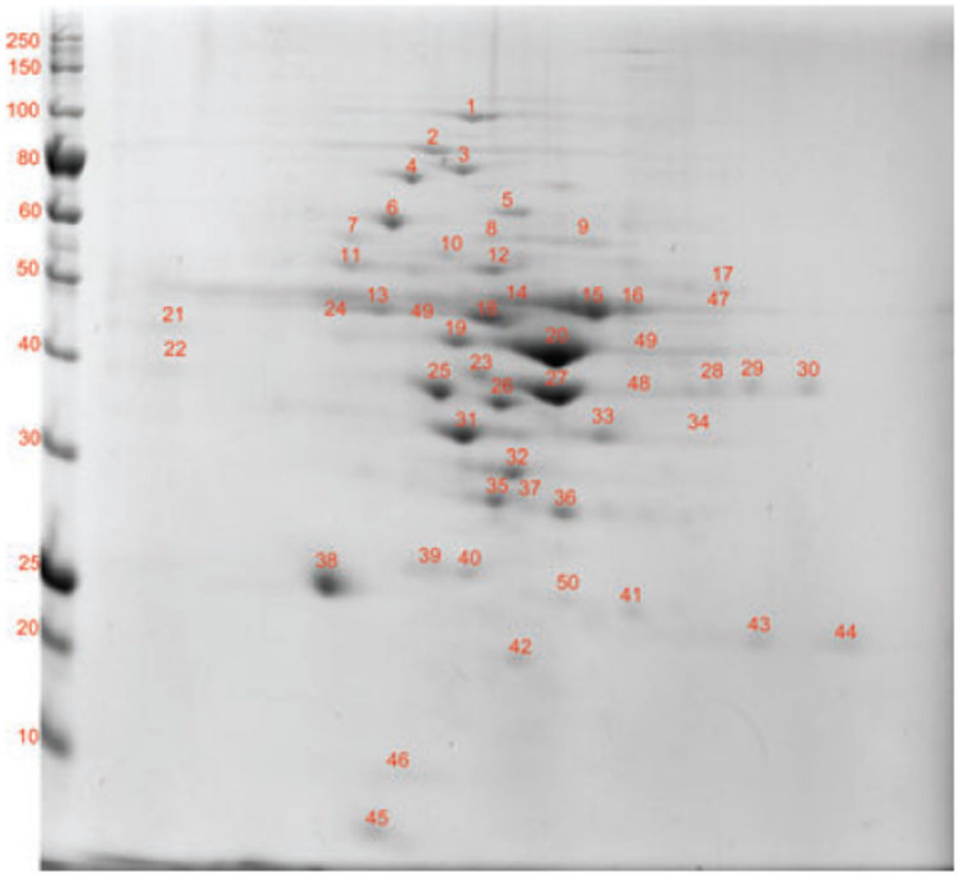

Figure 3.

2D-PAGE of the membrane fraction of *F. alocis* ATCC 35896 strain. 2D page was performed using 7-cm IPG strips of p*I* 3–10 in Protean IEF cell and 30–50 μg of protein and electrophoresed at 200 V, 0.3 A for 4–5 h, and stained with Coomassie simply blue strain. A total of 50 distinct spots were identified and processed for MS/MS analysis.

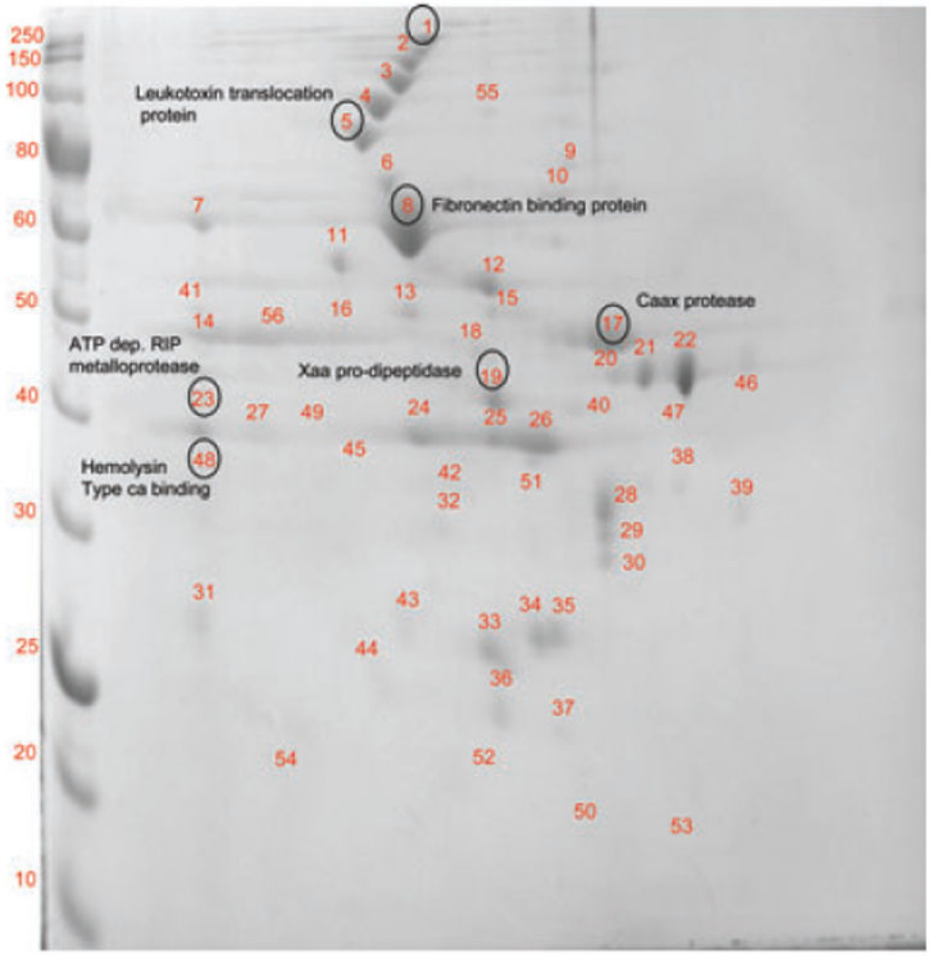

Figure 4.

2D-PAGE of the membrane fraction of *F alocis* D-62D strain. 2D page was performed using 7-cm IPG strips of p*I* 3–10 in Protean IEF cell and 30–50 μg of protein and electrophoresed at 200 V, 0.3 A for 4–5 h and stained with Coomassie simply blue strain. A total of 54 distinct spots were identified and processed for MS/MS analysis.

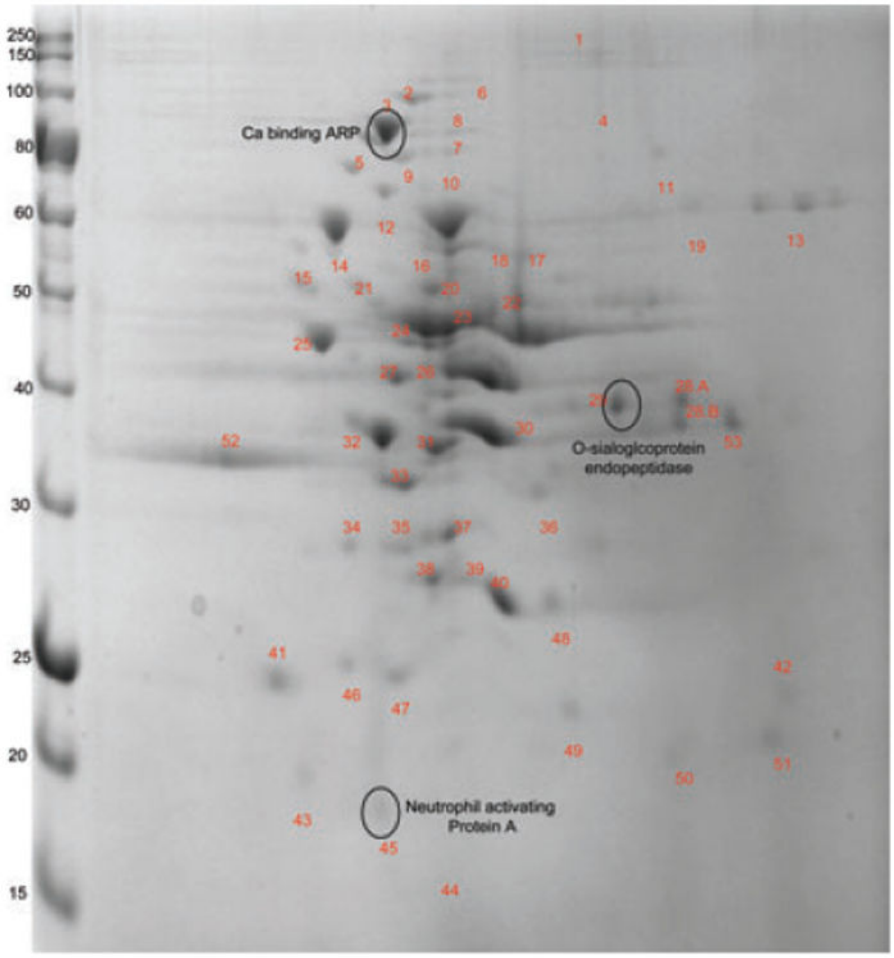

Figure 5.

2D-PAGE of the extra-cellular fraction of *F. alocis*–ATCC-35896 strain. 2D page was performed using 7 cm IPG strips of p*I* 3–10 in Protean IEFcell and 30–50 μg of protein and electrophoresed at 200 V, 0.3 A for 4–5 h, and stained with Coomassie simply blue strain. A total of 55 distinct spots were identified and processed for MS/MS analysis.

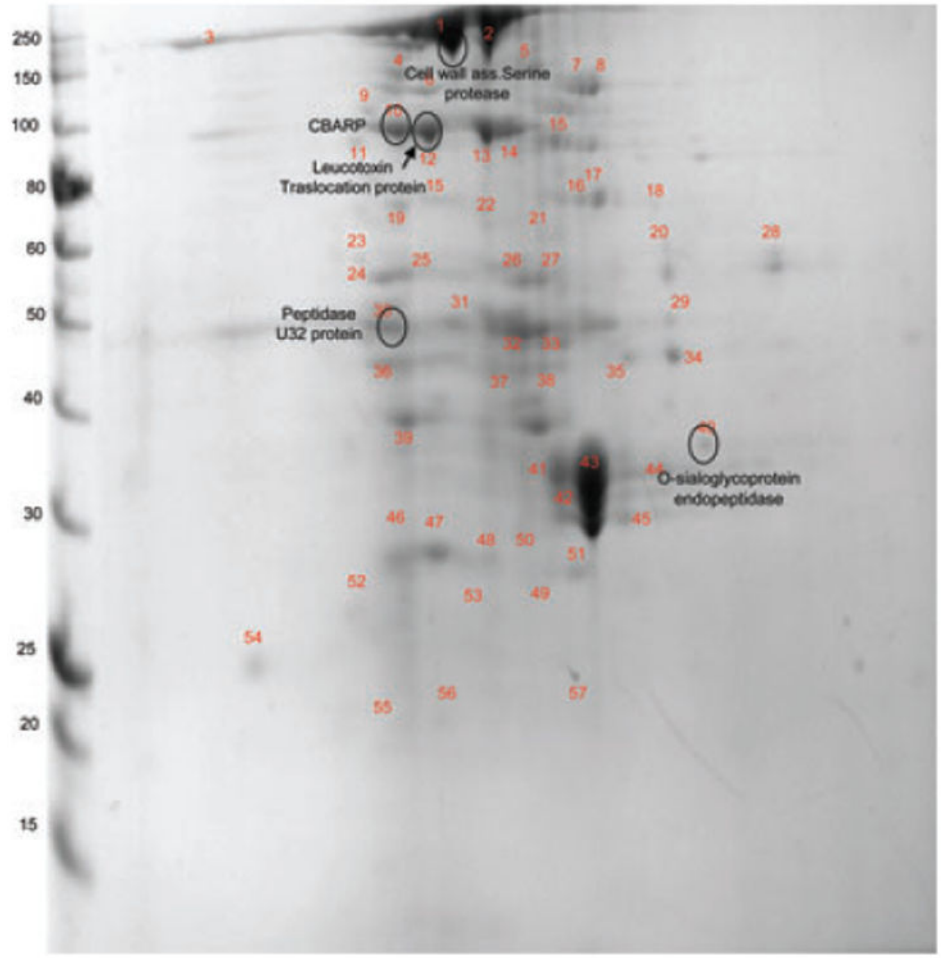

Figure 6.

2D-PAGE of the extra-cellular fraction of *F. alocis* D-62D strain. 2D page was performed using 7-cm IPG strips of pI 3–10 in Protean IEF cell and 30–50 μg of protein and electrophoresed at 200 V, 0.3 A for 4–5 h, and stained with Coomassie simply blue strain. A total of 60 distinct spots were identified and processed for MS/MS analysis.

Table 1

***F. alocis* AJCC 35896 — membrane fraction**

Spot	Accession[a)]	Protein description[a)]	Mol. wt/Calculated mol. wt (kDa)	PMF Score[b)]/(em PAI)	Total peptides matched[c)]	PSORT prediction score and category[d)]	Domains[e)]	HI score[f)]	Nature of protein[g)]
1.	HMPREF0389_01740	Hypothetical protein	104.4/104.3	35/0.09	5	0.243 CM	SecA ATPase domain	−0.56	Nonsecretory protein
2.	HMPREF0389_00724	ATP-dependent chaperone protein (ClpB)	97.5/97.6	14.98/1.85	82	0.380 CM	AAA domain (ATP associated with wide cellular activity)	−0.85	Nonsecretory protein
3.	HMPREF0389_01580	Leucotoxin translocation ATP-binding protein LktB	81/81.15	56/0.98	5	0.455 M	Four TMMH Domain P-loop NTPase domain	0.78	Cleavage site with no N terminal signal sequence
4.	HMPREF0389_00784	Copper amine oxidase N-domain protein	80/94.2	27/0.05	6	0.227C 0.112M	No conserved domain	−0.19	Nonsecretory protein
5.	HMPREF0389_00575	Fibronectin-binding protein	68.3/68.3	22/0.11	12	0.421 CM	N terminal fibronectin-binding domain with prokaryotes	−0.56	Nonsecretory protein
6.	HMPREF0389_00021	Hypothetical protein	70/69.2	76/0.63	8	2.356 C 0.114M	DUF 2156 uncharacterized conserved domain	−0.56	Nonsecretory protein
7.	HMPREF0389_00233	TraG family protein	66.7/66.8	23/0.32	4	0.238 M	Two TMMH domain	3.23	N terminal signal sequence Secretory protein
8.	HMPREF0389_00426	Type IV pilus assembly protein (PilB)	61/61.51	25	7	0.274 C 0.111 CM	Bacterial type II secretion system protein E signature domain	−0.12	Nonsecretory protein
9.	HMPREF0389_00804	Periplasmic Oligo peptide binding protein	60/60.3	106/0.31	14	0.640 CM	ABC type transporter signal domain	2.26	N terminal cleavage site. Possible lipoprotein transporter
10.	HMPREF0389_01305	Chaperonin GroL	57.7/60	2327/4.90	130	4.213 C 0.065 M	Type-I chaperonin doman	−0.19	Nonsecretory protein
11.	HMPREF0389_00773	Amino acyl histidine dipeptidase	55/54.8	41/0.29	4	3.927 C 0.964 M	M20 peptidase D domain	0.41	Nonsecretory protein
12.	HMPREF0389_01130	Fe hydrogenase large subunit family protein	55.5/54.8	71/0.08	3	0.251C 0.284 M	Iron hydrogenase domain	0.89	Nonsecretory protein
13.	HMPREF0389_01643	Hypothetical protein	53/53.37	25/0.08	4	0.120 CM	No conserved domains identified	1.85	N terminal signal peptide Secretory protein
14.	HMPREF0389_01385	Mg chelate like protein-magnesium transporter	52.8/52.4	113/0.09	8	0.489 M	Five TMMH domains Divalent cation transporter domain	−0.19	Weak cleavage site with no N terminal signal peptide
15.	HMPREF0389_00816	Signal recognition particle protein	49.7/49.8	22/0.07	27	0.483 CM	SRP-Signal peptide binding domain	−0.45	Nonsecretory protein
16.	HMPREF0389_01719	Hypothetical protein	48.9/48.5	41/0.07	5	0.168 CM	Bacterial trigger factor C terminus domain	−0.11	Nonsecretory protein
17.	HMPREF0389_01646	Trigger factor	48.5/48.6	41/0.09	5	0.168 CM	Ribosome-associated trigger factor domain	0.23	Nonsecretory protein
18.	HMPREF0389_00590	Caax amino protease family	47/47.15	75/0.16	6	0.579 CM	Eight TMMH domains Caax protease—self-immunity domain	−0.75	Cleavage site with no N terminal signal sequence
19.	HMPREF0389_01716	Hypothetical protein	47.2	25/0.09	5	0.215 M	Glutamate DH multi domain	−0.78	Nonsecretory protein

Spot	Accession[a)]	Protein description[a)]	Mol. wt/Calculated mol. wt (kDa)	PMF Score[b)]/ (em PAI)	Total peptides matched[c)]	PSORT prediction score and category[d)]	Domains[e)]	HI score[f)]	Nature of protein[g)]
20.	HMPREF0389_01584	Arginine deaminase	46.6/46.5	247/0.54	27	2.31 C 0.193 M	Amidotransferase domain	1.85	Nonsecretory protein
21.	HMPREF0389_01173	Dehydrogenase/methenyl tetrahydrofolate cyclohydrolase	49/49.5	41/0.11	8	2.135C 0.129M	Tetrahydrofolate catalytic domain	0.89	Nonsecretory protein
22.	HMPREF0389_00745	Acetyl coA acetyl transferase	41/41.3	819/1.74	54	4.235 C 0.110M	Thiolase domain	−0.89	Nonsecretory protein
23.	HMPREF0389_01570	Acetyl ornithine transaminase	43.9/44	550/1.22	52	0.203 C 0.432 CM	AAT superfamily domain	0.89	Nonsecretory protein
24.	HMPREF0389_00225	Transcriptional regulatory protein	48.3/47.9	64/0.09	5	0.128 CM	No conserved domains	−0.68	Nonsecretory protein
25.	HMPREF0389_00021	Hypothetical protein	37.3/37.2	41/0.11	5	0.425C 0.056CM	DUF 2156 domain	−0.23	Nonsecretory protein
26.	HMPREF0389_00599	Hypothetical protein	39.5/39.2	24/0.24	4	3.872 M	Five TMMH domains	1.74	N terminal signal sequence Secretory protein
27.	HMPREF0389_01692	Hypothetical protein	44/44.2	908/1.75	53	0.298 C 0.123 CM	Translation elongation factor domain	−0.56	Nonsecretory
28.	HMPREF0389_01658	Acetate kinase	43.7/43	80/0.16	6	0.106 C 0.056 M	Acetate kinase domain	−0.35	No signal sequence
29.	HMPREF0389_01707	Hypothetical protein	42.5/42.3	80/0.16	6	1.12 C 0.89 M	Acetate kinase domain	0.12	Nonsecretory protein
30.	HMPREF0389_01733	Hypothetical protein	44/43.98	201/0.24	16	3.21 C 0.11 M	Translation elongation factor domain	−0.19	Nonsecretory protein
31.	HMPREF0389_01077	Dihydrodipicolinate reductase	37/38.01	21/0.11	3	2.31 C 0.239 M	Dehyrogenase domain	0.78	Nonsecretory protein
32.	HMPREF0389_00704	TRAP transporter solute receptor—TAXI family	36/35.9	47/0.31	9	0.119M	One TMMH domain	0.36	N terminal signal peptide Secretory protein
33.	HMPREF0389_00145	TIM —barrel protein	36.2/36.15	38/0.09	5	3.564 C 0.117 M	Phosphate-binding domain	−0.56	Nonsecretory protein
34.	HMPREF0389_00742	Electron transfer flavoprotein alpha subunit protein	35/35.1	246/0.43	15	0.160 M	ETF electron acceptor domain	−0.56	Nonsecretory protein
35.	HMPREF0389_01141	Hypothetical protein	30/30	24/0.11	9	4.65 C 0.362 M	No conserved domain	−	Nonsecretory protein
36.	HMPREF0389_01354	NG, NG dimethyl arginine, dimethyl amino hydrolase	29/29.2	48/0.11	5	2.568 C 0.116 M	Amidotransferase domain	−0.36	Nonsecretory protein
37.	HMPREF0389_00553	Septum site determining protein MinD	29/29.5	55/0.11	3	0.126 M	Membrane-associated ATPase domain	−0.56	Nonsecretory protein
38.	HMPREF0389_01240	3-Oxy acyl carrier protein Amino acid carrier protein	27.5/28	341/1.23	19	0.747 M	Eight TMMH domains	0.45	Uncleavable N terminal signal sequence
39.	HMPREF0389_00128	GTP sensing transcriptional pleotropic repressor CodY	28/28.4	72/0.40	7	0.374 C 0.089 M	GAF-like domain (found to repress the dipeptide transport operon)	0.36	Nonsecretory protein

Spot	Accession[a)]	Protein description[a)]	Mol. wt/Calculated mol. wt (kDa)	PMF Score[b)]/ (em PAI)	Total peptides matched[c)]	PSORT prediction score and category[d)]	Domains[e)]	HI score[f)]	Nature of protein[g)]
40.	HMPREF0389_01469	Glutaconate coA transferase	29.5/30	1385/7.46	191	0.110C 0.056 M	CoA tranferase domain	−0.51	Nonsecretory protein
41.	HMPREF0389_01209	Ruberythrin	21.4/21.6	48/0.34	10	4.84 C 0.213 M	Ferritin-like di iron binding domain	−0.65	Nonsecretory protein
42.	HMPREF0389_01167	CRISPR-associated protein	18./20.1	22/3.9	16	3.56 C 0.251 M	CRISPR domain (clustered regularly interspaced short palindromic repeats)	−0.36	Nonsecretory protein
43.	HMPREF0389_01230	Hypothetical protein	22/22.02	123/1.06	13	0.447 CM	No conserved domain	0.11	Nonsecretory protein
44.	HMPREF0389_00682	CBS domain protein	23.5/23.7	38/0.40	6	3.61 C 0.197 M	CBS-Bateman domain	0.12	Nonsecretory protein
45.	HMPREF0389_00796	Superoxide reductase	12.5	53/0.56	3	4.235 C 1.89 M	SOR-like domain	−0.45	Nonsecretory protein
46.	HMPREF0389_00708	Alkaline shock protein	14/14.02	80/0.24	3	0.175 C 0.052 M	DUF322 domain	0.36	Nonsecretory protein
47.	HMPREF0389_00532	D-Alanine–D-alanine ligase	40/40.3	45/0.330	10	3.21 C 0.112 M	Substrate binding LTTR domain	0.89	Nonsecretory protein
48.	HMPREF0389_00019	Membrane protein	37.8/36.2	32/0.31	7	0.703 CM	TMMH domain	−0.78	Nonsecretory protein
49.	HMPREF0389_00429	Serine-glucine-hydroxymethyl transferase	47/46.9	24/0.09	7	2.123 C 0.075 M	SHMT domain	−0.48	Nonsecretory protein
50.	HMPREF0389_00639	ATP/GTP-binding protein	28/32.2	120/0.09	10	0.348 CM	Protein transfer/ATP-GTP binding domain	1.85	Nonsecretory protein

[a)] Accession numbers and protein descriptions are from the NCBI- *F alocis* genome project (http://www.ncbi.nlm.nih.gov/genomeprj/46625).

[b)] Peptide mass fingerprinting score from Mascot.

[c)] Number of matched peptides derived from Mascot.

[d)] Psort prediction score classifying protein as C, cytoplasmic; CM, cytoplasmic membrane; M, membrane; CW, cell wall; PP, periplasm; Ex, extra cellular.

[e)] Conserved domain prediction using the NCBI-Conserved domain database search.

[f)] Hydropathy index (HI) score from the iPsort predictions on the nature of protein, high positive score indicate presence of a signal sequence negative scores predict proteins as nonsecretory.

[g)] iPsort prediction showing protein to contain signal sequence, cleavage site and classification of protein to be secretory or nonsecretory.

Table 2

***F. alocis* D-62 D—membrane fraction**

Spot	Accession[a)]	Protein description[a)]	Mol. wt/Calculated mol. wt (kDa)	PMF score[b)]/(emPAI)	Total peptides matched[c)]	PSORT prediction score and category[d)]	Domains[e)]	HI score[f)]	Nature of protein[g)]
1.	HMPREF0389_01532	Calcium-binding acid repeat proteins	205/209	21/19.8	2	4.23 C 0.112 M	Lipase domain	1.785	N terminal signal sequence
2.	HMPREF0389_01139	S-layery domain containing protein	140/147	89/89.2	17	0.300 M	SLH domain	1.167	Signal peptide Cleavage protein
3.	HMPREF0389_00555	Peptidoglycan biosynthesis transpeptidase	107/107.7	41/0.39	5	2.104 M	Pencillin-binding protein transpeptidase domain	3.25	Uncleavable N terminal signal peptide sequence
4.	HMPREF0389_01225	Copper amine oxidase N domain protein	80.2/80.3	25/0.06	6	3.00 CW/M	N terminal copper amine oxidase domain	2.75	Cleavable N terminal signal sequence Secretory protein
5.	HMPREF0389_01580	Leucotoxin translocation ATP-binding protein LktB	81/81.15	71/0.91	5	0.455 M	Four TMMH domain P loop NTPase domain	0.78	Cleavage site with no N terminal signal sequence
6.	HMPREF0389_01693	Hypothetical protein	75/75.1	25/0.12	4	0.232C	Two TMMH domains	2.35	Uncleavable N terminal signal sequence Secretory protein
7.	HMPREF0389_01750	Hypothetical protein	71/69.8	30/0.05	8	3.10 C	Collagen binding protein B domain	0.12	Nonsecretory protein
8.	HMPREF0389_00575	Fibronectin-binding protein	68.3/68.3	20/0.11	10	0.421 CM	N terminal fibronectin-binding domain with prokaryotes	−0.56	Nonsecretory protein
9.	HMPREF0389_00239	Peptidase M23/M37 family	69.8/69.9	23/0.33	5	2.37 M	NlpC/P60 family Lipoprotein domain	−0.63	Non classical secretory protein[h)]
10.	HMPREF0389_00416	Type IV pilus assembly protein	65/64.8	24/0.07	2	3.65 C 1.230 M	Tfp pilus assembly protein domain		Nonsecretory protein
11.	HMPREF0389_00926	Oligo endo peptidase F	65.7/65.9	22/0.56	2	4.37 C 0.128 M	Peptidase family M3B domain	0.23	Nonsecretory protein
12.	HMPREF0389_00804	Periplasmic oligo peptide binding protein	60.3/60.1	106/0.31	14	0.640 CM	ABC type transporter signal domain	2.26	N terminal cleavage site. Possible lipoprotein transporter
13.	HMPREF0389_00773	Amino acyl histidine dipeptidase	55/54.8	41/0.29	4	3.927 C 0.964 M	M20 peptidase D domain	0.41	Nonsecretory protein
14.	HMPREF0389_01064	Amino acid carrier protein	50.8/50.2	125/0.09	18	4.789 M	Nine TMMH domainsSodium: alanine symporter family domain	−0.98	Nonsecretory protein
15.	HMPREF0389_01173	Dehydrogenase/methenyl tetrahydrofolate cyclohydrolase Bifunctional protein GlmU	49/49.5	42/0.10	9	2.135 C 0.129M	Tetrahydrofolate catalytic domain	−0.75	Nonsecretory protein
16.	HMPREF0389_01385	Mg chelate like protein-magnesium transporter	52.8/53	124/0.12	9	0.489 M	Five TMMH domains Divalent cation transporter domain	−0.19	Weak cleavage site with no IM terminal signal peptide
17.	HMPREF0389_00590	Caax amino protease family	47/47.15	127/0.07	15	0.579 CM	Eight TMMH domains Caax protease-self-immunity domain	−0.75	Cleavage site with no N terminal signal sequence
18.	HMPREF0389_01276	Iron permease FTR1 family	47.4/47	52/7.4	6	4.286 M	Six TMMH domainsFTR1 domain	2.29	Cleavable N terminal signal sequence Secretory protein

Spot	Accession[a)]	Protein description[a)]	Mol. wt/Calculated mol. wt (kDa)	PMF score[b)]/(emPAI)	Total peptides matched[c)]	PSORT prediction score and category[d)]	Domains[e)]	HI score[f)]	Nature of protein[g)]
19.	HMPREF0389_01538	Xaa pro dipeptidase	42/39.8	75/0.16	6	4.491 C 0.477 M	Metallopeptidase family M24 (play roles in regulation of biological processes rather than general protein degradation)	0.12	Nonsecretory protein
20.	HMPREF0389_00799	Signal peptidase (amino peptidase l family)	42.6/42.2	39/0.32	6	4.673 M	Eight TMMH domains	−0.84	Nonsecretory protein
21.	HMPREF0389_01222	Hypothetical protein	44/43.5	27/0.23	17	4.302 C 0.470 M	Metal-dependent hydrolase domain	−0.12	Nonsecretory protein
22.	HMPREF0389_01570	Acetyl ornithine transaminase	43.9/44	208/0.59	15	0.203C 0.432CM	AAT superfamily domain	0.89	Nonsecretory protein
23.	HMPREF0389_00112	ATP-dependent RIP metalloprotease	38.3/38.1	85/7.3	8	4.501 M	Three TMMH domains PDZ metalloprotease domain	2.96	Cleavable N terminal signal sequence Secretory protein
24.	HMPREF0389_00090	Heat inducible transcr858iptional repressor protein	39.7/39.76	21/0.11	3	3.59 C 1.35 M	HrcA protein C domain (negatively regulate the transcription of heat shock qenes)	−0.56	Nonsecretory protein
25.	HMPREF0389_00672	Hypothetical protein	38.7/38.5	21/0.84	4	4.375 M	Five TMMH domain	0.74	Nonsecretory protein
26.	HMPREF0389_00599	Hypothetical protein	39.5/39.2	24/0.24	4	3.872 M	Five TMMH domains	1.74	N terminal signal sequence Secretory protein
27.	HMPREF0389_01104	Hypothetical protein	38.3/38.4	21/0.32	6	2.39 C 1.36 M	DHH family domain	−0.36	Nonsecretory
28.	HMPREF0389_00019	Membrane protein	37.8/36.2	28/0.25	5	1.102 M 2.838 Ex	TMMH domain	−0.78	Nonsecretory protein
29.	HMPREF0389_00858	Pyridoxine biosynthesis protein	30/30.27	22/0.14	4	4.836 C 0.148 M	No conserved domain	−0.63	Nonsecretory protein
30.	HMPREF0389_01354	NG, NG dimethyl arginine, dimethyl amino hydrolase	29/29.2	48/0.11	5	2.568 C 0.116 M	Amidotransferase domain	−0.36	Nonsecretory protein
31.	HMPREF0389_01172	Hypothetical protein	27.52/27.3	38/0.24	4	4.251 M	Six TMMH domains membrane transporter domain protein	−0.74	Nonsecretory protein
32.	HMPREF0389_00639	ATP/GTP-binding protein	28/32.2	26/0.62	3	0.348 CM	Protein transfer/ATP-GTP binding domain	−1.09	Nonsecretory
33.	HMPREF0389_01587	Aspartate racimase	26.3/26.4	25/0.13	4	3.018 C 1.706 M	Aspartate racemase multidomain	−0.12	Nonsecretory protein
34.	HMPREF0389_00107	UMP kinase	25.6/25.1	24/0.13	6	4.580 C 0.365 M	UMPK domain	−0.56	Nonsecretory protein
35.	HMPREF0389_01594	GTP pyrophospokinase	27.1/27.3			4.535 C 0.428 M	Nucleotidyl transferase (NT) domain	−	Nonsecretory protein
36.	HMPREF0389_00415	Fimbrial assembly protein PilN	25.9/26.1	32/0.71	5	3.37 C 1.15M	Fimbrial assembly protein domain	0.12	Nonsecretory protein
37.	HMPREF0389_01157	Hypothetical protein	19/19.4	27/0.23	3	4.667 C 0.115M	DUF 1877 domain	−0.56	Nonsecretory protein
38.	HMPREF0389_01657	Membrane protein	37.5/36.8	22	2	0.442 CM	Six TMMH domains and precursor signal inner protein domain	1.366	N terminal cleavage signal

Spot	Accession[a)]	Protein description[a)]	Mol. wt/Calculated mol. wt (kDa)	PMF score[b)]/ (emPAI)	Total peptides matched[c)]	PSORT prediction score and category[d)]	Domains[e)]	HI score[f)]	Nature of protein[g)]
39.	HMPREF0389_00742	Electron transfer flavoprotein alpha subunit protein	35/35.1	246/0.43	15	0.160 M	ETF electron acceptor domain	−0.56	Nonsecretory protein
40.	HMPREF0389_00637	NLP/P60 family protein	27/36.1	22/0.45	4	3.860 CM	Lipoprotein domain	2.35	N terminal signal sequence Secretory protein
41.	HMPREF0389_00816	Signal recognition particle protein	49.7/49.8	21/0.25	25	0.483 CM	SRP signal peptide binding domain	−0.45	Nonsecretory protein
42.	HMPREF0389_01566	Oligo peptide/dipeptide ABC transporter substrate/ATP binding protein	31.3/31	78/7.42	16	2.175 M	Copper amine oxidase N terminal domain	2.87	A gram positive N terminal signal peptide sequence Secretory protein
43.	HMPREF0389_00768	Peroxiredoxin	20/19.9	26/0.36	6	4.129 C 0.490 M	Thiol specific antioxidant domain	−0.65	Nonsecretory protein
44.	HMPREF0389_01476	Hypothetical protein	20.1/20	48/0.42	4	1.973 M	DUF 1836 uncharacterized domain	−0.78	Nonsecretory
45.	HMPREF0389_00295	Ribose ABC transporter, periplasmic ribose binding protein	32/32.4	65/0.56	6	0.300 M	Periplasmic binding fold domain	2.84	N terminal signal peptide sequence
46.	HMPREF0389_01217	Hypothetical protein	37.3/37	21/0.09	4	3.837 C 1.038 M	ParB-like nuclease domain	−0.68	Nonsecretory protein
47.	HMPREF0389_01478	Protein export membrane protein	35/35.3	21/0.09	4	4.754 M	Nine TMMH domains SecD and SecF domain	3.23	N terminal signal peptide sequence
48.	HMPREF0389_01477	Hemolysin III type calcium-binding protein.	31/31.1	32/1.01	6	4.807 M	Six TMMH Domains-Hemolysin –III domain	−0.23	Nonsecretory
49.	HMPREF0389_00894	Zinc ABC transporter periplasmic zinc binding protein	34.1/34.3	54/5.2	7	4.811 C 0.105 M	Periplasmic solute binding protein domain	2.84	Cleavable N terminal signal sequence Secretory protein
50.	HMPREF0389_00243	Toxin antitoxin component, ribbon —helix-helix fold protein	10.6/10.5	45/1.03	5	3.913 C 0.509 PP	RelB antitoxin domain	0.11	Nonsecretory
51.	HMPREF0389_01445	O-Sialoglycoprotein endopeptidase.	36.6/36.2	22/0.55	5	1.806 C 1.17 M	Metal-dependent protease–molecular chaperone domain	−0.45	Potent cleavage site without IM terminal signal sequence
52.	HMPREF0389_01654	Neutrophil-activating factor protein A	14/16.2	29/0.56	2	2.310 C 0.099 M	DPS domain	0.32	Nonsecretory
53.	HMPREF0389_01030	Hypothetical protein	15.6/15.9	24/0.22	4	4.662 C 0.103 M	No conserved domain	−0.41	Nonsecretory
54.	HMPREF0389_00964	Ferric uptake regulatory protein	17/17.2	21/0.32	4	3.74 C 0.820 M	Iron-dependent DNA binding reporessor/activator domain	−0.88	Nonsecretory protein
55.	HMPREF0389_ 01266	Cation transporting ATPase	99.7/99.76	49/0.72	6	2.781 M	C terminus cation transporting ATPase domain	−0.41	Nonsecretory protein
56.	HMPREF0389_01748	Hypothetical protein	52/52.1	26/0.32	4	2.489 M	Anion permease transmembrane domain	2.67	Potent cleavage site without IM terminal signal sequence

[a)] Accession numbers and protein descriptions are from the NCBI *F alocis* genome project (http://www.ncbi.nlm.nih.gov/genomeprj/46625).

[b)] Peptide mass fingerprinting score from Mascot.

[c)] Number of matched peptides derived from Mascot.

[d)] Psort prediction score classifying protein as: C, cytoplasmic; CM, cytoplasmic membrane; M, membrane; CW, cell wall; PP, periplasm; Ex, extra cellular.

[e] Conserved domain prediction using the NCBI-Conserved domain database search.

[f] Hydropathy index (HI) score from the iPsort predictions on the nature of protein, high positive score indicate presence of a signal sequence negative scores predict proteins as nonsecretory.

[g] iPsort prediction showing protein to contain signal sequence, cleavage site and classification of protein to be secretory or non-secretory,

[h] Nonclassical secretory protein in silico prediction through "Secretome."

Table 3

***F. alocis* AJCC 35896 — extracellular fraction**

Spot	Accession[a)]	Protein description[a)]	Mol. wt/Calculated mol. wt (kDa)	PMF score[b)]/(emPAI)	Total peptides matched[c)]	PSORT prediction score and category[d)]	Domains[e)]	HI score[f)]	Nature of protein[g,h)]
1.	HMPREF0389_01419	Conserved hypothetical protein	145.4	32/0.39	4	C-7.50 EC-0.73	DNA—ATP-binding domain	–	Nonsecretory
2.	HMPREF0389_01687	Pyruvate-flavodoxin oxidoreductase	130	24/0.07	2	C-7.50 EC-0.73	4 Fe-4S ferredoxin-type iron-sulfur binding domain	1.86	N terminal signal peptide
3.	HMPREF0389_01448	Calcium-binding acid repeat protein	103	34/0.42	6	Unknown	SLH domains —3 numbers	2.0	N terminal signal peptide
4.	HMPREF0389_01431	Conserved hypothetical protein	97.5	71/0.92	5	EC -2.92	Precursor signal domain	1.02	N terminal signal sequence
5.	HMPREF0389_00279	ATP-dependent protease La	87.9	22/0.12	4	C-9.97 EC-0.02	Serine protease La binding domain	–	Nonsecretory
6.	HMPREF0389_000638	Membrane protein	80.45	23/0.33	7	M	Membrane protein precursor signal	–	Nonsecretory
7.	HMPREF0389_01452	Conserved hypothetical protein	76.8	20/0.11	10	CM-9.8 EC-0.12	S-layer precursor signal domain	2.32	N terminal signal peptide
8.	HMPREF0389_01693	Conserved hypothetical protein	75.1	25/0.12	12	Unknown	GGDEF response regulatory domain	1.2	N terminal signal peptide
9.	HMPREF0389_01750	Hypothetical protein	71/69.8	30/0.05	8	3.10 C 1.05 M	Collagen binding protein B domain	–	Nonsecretory protein
10.	HMPREF0389_00315	Conserved hypothetical protein	70.7	28/0.07	6	C-7.50 EC-0.73	Secretory system-II pilus domain		Nonsecretory
11.	HMPREF0389_00575	Fibronectin-binding protein	68.1	34/0.32	7	C-7.50 EC-0.73	Protein A binding adherence fibronectin/fibrinogen domain	–	Nonsecretory
12.	HMPREF0389_00223	S layer Y containing domain	66.7	22/0.33	3	CW-9.2 EC-0.78	S layer homology domain	1.88	N terminal single peptide
13.	HMPREF0389_00803	Conserved hypothetical protein	63.8	24/0.07	3	Unknown	Histidine kinase domain	–	Nonsecretory
14.	HMPREF0389_01605	Formate tetra hydrofolate ligase	60.17	28/0.07	2	C-7.00 EC-0.73	FTH dignature domain	–	Nonsecretory
15.	HMPREF0389_00804	Oligopeptide-binding protein	60.25	32/0.11	4	EC-0.91	Lipid attachment domain at two positions	2.26	N terminal signal peptide
16.	HMPREF0389_00868	DAK 2 domain protein	58.8	22/0.07	2	C-7.50 EC-0.73	DhaL profile domain	–	Nonsecretory
17.	HMPREF038_00596	UDP-N –muramyl tripeptide synthetase	57.06	102/0.24	16	C-7.50	Cell wall tripeptide synthetase domain	–	Nonsecretory
18.	H22MPREF0389_00480	Amido transferase family protein	54.7	22/0.08	4	C-7.50 EC-0.73	GATB domain	–	Nonsecretory
19.	HMPREF0389_01130	Ferrous hydrogenase	54.3	51/0.16	12	C-7.5 EC-0.73	Ferrodoxin type Fe-S binding domain	1.88	N terminal signal peptide

Spot	Accession[a)]	Protein description[a)]	Mol. wt/Calculated mol. wt (kDa)	PMF score[b)]/ (emPAI)	Total peptides matched[c)]	PSORT prediction score and category[d)]	Domains[e)]	HI score[f)]	Nature of protein[g,h)]
20.	HMPREF0389_00225	Trancriptional regulatory protein	48	84/0.18	17	C-7.5 EC-0.73	No conserved domains	–	Nonsecretory
21.	HMPREF0389_01374	Conserved hypothetical protein	48.5	289/0.30	20	C-9.5 EC-0.2	YNIH-BH1805-YDJI domain		Nonsecretory
22.	HMPREF0389_00504	Peptidase U32 family protein	47.7	22/0.07	4	C-7.50 EC-0.73	Peptidase U 32 domain	–	Nonsecretory
23.	HMPREF0389_01584	Arginine deiminase	46.6	56/0.18	18	C-7.5 EC-0.73	Arginine deiminase domain	–	Nonsecretory
24.	HMPREF0389_01570	Acetyl ornithine transaminase	43.5	182/0.44	19	C-9.97 EC-0.02	AA transfer class 3 domain	–	Nonsecretory
25.	HMPREF0389_01465	Conserved hypothetical protein	41.5	55/0.16	8	C-7.5 EC-0.73	Hydrolase domain		Nonsecretory
26.	HMPREF0389_000744	Butryl coA dehydrogenase	41.25	64/0.16	12	C-7.50 EC-0.73	Acetyl coA DH1 and DH2 domain	–	Nonsecretory
27.	HMPREF0389_00745	Acetyl coA acetyl transfserase	40.9	78/0.15	32	C-7.2 EC-0.93	Thiolase 1,2,3 domain	–	Nonsecretory
28A.	HMPREF0389_01567	N acetyl gamma glutamyl phosphate reductase	38.7	212/0.56	20	Unknown	NAC gama glutamyl phosphate domain	–	Nonsecretory
28B.	HMPREF0389_00567	Glyceraldehyde 3 phosphate dehydrogenase	37.9/39.5	39/0.06	5	0.351 C	Nil	–	Nonsecretory
29.	HMPREF0389_01445	O-Sialoglycoprotein endopeptidase	36.6/36.2	248/0.65	24	1.806 C 1.17M	Metal-dependent protease—molecular chaperone domain	–0.45	Potent cleavage site without N terminal signal sequence
30.	HMPREF0389_00607	Conserved hypothetical protein	36.2	22/0.09	5	Unknown	Precursor signal domain	1.71	N terminal signal peptide
31.	HMPREF0389_00704	TRAP transporter solute receptor protein	35.9	35/0.12	6	Unknown	Lipoportein lipid attachment domain	1.12	N terminal signal peptide
32.	HMPREF0389_01401	Conserved hypothetical protein	34.9	32/0.09	7	EC-0.73	Precursor signal YQFA trans membrane domain	3.67	Strong N terminal signal peptide
33.	HMPREF0389_00901	Cobalt import ATP-binding protein	33.9-5.2		9	CM-8.73 EC-0.09	CBIO-ATP binding domain	–	Nonsecretory
34.	HMPREF0389_01489	Conserved hypothetical protein	32.3	67/0.25	7	Unknown	No conserved domains	2.21	Signal peptide at the N terminal
35.	HMPREF0389_01569	Acetyl glutamate kinase	31.03	42/0.08	7	EC-0.73	Arginine amino acid kinase		Nonsecretory
36.	HMPREF0389_01545	Copper amine oxidase N-domain protein	30.5	43/0.13	6	Unknown	Precursor signal domain	1.96	N terminal signal sequence
37.	HMPREF0389_01471	Glutaconyl coA decarboxylase	29.4	313/0.18	16	CM	Acetyl CoA CT- N and C terminal domains	–	Nonsecretory
38.	HMPREF0389_	Glutamate racemase	29.4	42/0.12	6	EC-0.75 C-3.45	Aspartate glutamate racemase signature	–	Nonsecretory
39.	HMPREF0389_00100	Septum site determining protein	28.9	306/0.84	17	CM	Septum site determining cell division inhibitor domain	28.9	N terminal signal peptide
40.	HMPREF0389_01597	Electron transfer flavoprotein beta	28.2	14/0.07	2	EC-0.73 C-6.32	ET-Flavoprotein beta domain	–	Nonsecretory
41.	HMPREF0389_01177	Conserved hypothetical protein	27.1	45/0.14	6	Unknown	No conserved domains	–	

Spot	Accession[a)]	Protein description[a)]	Mol. wt/Calculated mol. wt (kDa)	PMF score[b)]/ (emPAI)	Total peptides matched[c)]	PSORT prediction score and category[d)]	Domains[e)]	HI score[f)]	Nature of protein[g,h)]
42.	HMPREF0389_01259	Histidinol phosphatase	25.2-6.36	32/0.11	4	C-7.50 EC-0.73	PHP-C terminal domain	–	Nonsecretory
43.	HMPREF0389_01071	Tetracyclin resistant protein	20.8-6.35	59/0.13	11	C-7.50 EC-0.73	No conserved domain	–	Nonsecretory
44.	HMPREF0389_01503	Conserved hypothetical protein	15.7-9.1	43/0.11	10	Unknown	No conserved domain	–	Nonsecretory
45.	HMPREF0389_01654	Neutrophil-activating factor protein A	14/16.2	33/0.12	8	2.310 C 0.099 M	DPS domain	0.32	Nonsecretory
46.	HMPREF0389_01741	Conserved hypothetical protein	8.7-9.4	12/0.04	2	Unknown	No conserved domain	–	Nonsecretory
47.	HMPREF0389_01594	GTP pyrophosphokinase	25.1/26.8	28/0.07	2	0.244 C	GTP kinase domain	–0.84	Nonsecretory
48.	HMPREF0389_ 01239	Hypothetical protein	23/27.3	69/0.10	2	0.094 C	None	1.833	Signal peptide Lipoprotein cleavage signal
49.	HMPREF0389_01176	N-acetylmuramoyl-L-alanine amidase	27	16/0.09	4	Multiple localization	Autolysin precursor signal domain		Nonsecretory
50.	HMPREF0389_00927	Hypothetical protein	23.9	11/0.03	2	C-7.5 EC-0.73	Unknown	–	Nonsecretory
51.	HMPREF0389_01268	3H domain protein	20.5	22/0.07	2	C-7.5 EC-0.73	Biotin 3H domain	–	Nonsecretory
52.	HMPREF0389_00921	Thioredoxin family protein	33.2	12/0.07	2	Multiple localization	Reductase peptide methionine		Nonsecretory
53.	HMPREF0389_00877	Radical SAM domain containing protein	36	11/0.06	4	C-7.5 EC-0.73	Oxidoreductase SAM domain	–	Nonsecretory

a) Accession numbers and protein descriptions are from the NCBI *F alocis* genome project (http://www.ncbi.nlm.nih.gov/genomeprj/46625).

b) Peptide mass fingerprinting score from Mascot.

c) Number of matched peptides derived from Mascot.

d) Psortb prediction score classifying protein as: C, cytoplasmic; CM, cytoplasmic membrane; M, membrane; CW, cell wall; PP, periplasm; Ex, extra cellular.

e) Conserved domain prediction using the NCBI-Conserved domain database search.

f) Hydropathy index (HI) score from the iPsort predictions on the nature of protein, high positive score indicate presence of a signal sequence negative scores predict proteins as non secretory.

g) iPsort prediction showing protein to contain signal sequence, cleavage site and classification of protein to be secretory or non-secretory,

h) Nonclassical secretory protein in silico prediction through “Secretome.”

Table 4

***F. alocis* D-62D— extracellular fraction**

Spot	Accession[a)]	Protein description[a)]	Mol. wt/Calculated mol. wt (kDa)	PMF score[b)]/ (emPAI)	Total peptides matched[c)]	PSORT prediction score and category[d)]	Domains[e)]	HI score[f)]	Nature of protein[g)]
1.	HMPREF0389_01110	Cell wall associated serine proteinase	262	29/0.01	32	CM-9.39 EC-0.61	Membrane lipid attachment domain	1.61	N terminal signal peptide
2.	HMPREF0389_01728	Conserved hypothetical protein	246.5	25/0.04	4	EC-4.32 CW-5.69	Peptidoglycan anchor domain	1.37	N terminal signal peptide
3.	HMPREF0389_01692	Hypothetical protein	223	98/0.16	4	C-7.50 EC-0.73	Hemolysin III type calcium-binding signature domain Inorganic pyrophosphate domain	–	Nonsecretory
4.	HMPREF0389_01419	Conserved hypothetical protein	145.2	43/0.11	7	C-7.5 EC-0.73	DNA-binding domain	–	Nonsecretory
5.	HMPREF0389_01687	Pyruvate-flavodoxin oxidoreductase	130	156/0.29	45	C-7.50 EC-0.73	4 Fe-4S ferredoxin-type iron–sulfur binding domain	1.86	N terminal signal peptide
6.	HMPREF0389_01448	Calcium-binding acid repeat protein	103	25/020	16	Unknown	SLH domains-3 numbers	2.0	N terminal signal peptide
7.	HMPREF0389_00724	ATP-dependent chaperone protein	97.5	902/0.68	45	C-9.97 EC-0.02	Chaperonin cIpA/B signature domain	–	Nonsecretory
8.	HMPREF0389_01431	Conserved hypothetical protein	97.5	21/0.07	4	EC-2.92	Precursor signal domain	1.02	N terminal signal sequence
9.	HMPREF0389_00122	Protease	88.5	32/0.10	7	EC-0.73	Peptidase collagenase family domain	–	Nonsecretory
10.	HMPREF0389_00279	ATP-dependent protease La	87.9	26/0.07	5	C-9.97 EC-0.02	Serine protease La binding domain	–	Nonsecretory
11.	HMPREF0389_000638	Membrane protein	80.45	18/0.11	6	M	Membrane protein precursor signal	–	
12.	HMPREF0389_01580	Leucotoxin translocation ATP-binding protein	81.1	59/0.09	8	CM-10	Peptidase C-39, ABC transporter 2 domains	–	Nonsecretory
13.	HMPREF0389_01452	Conserved hypothetical protein	76.8	12/0.05	3	CM-9.87 EC-0.03	S-layer precursor signal domain	2.32	N terminal signal peptide
14.	HMPREF0389_01452	Conserved hypothetical protein	76.8	16/0.07	3	CM-9.8 EC-0.12	S-layer precursor signal domain	2.32	N terminal signal peptide
15.	HMPREF0389_01750	Hypothetical protein	71/69.8	22/0.05	8	3.10C 1.05 M	Collagen-binding protein B domain	0.12	Nonsecretory protein
16.	HMPREF0389_00315	Conserved hypothetical protein	70.7	138/0.08	6	C-7.5 EC-0.75	Secretory system-2 pilus domain	–	Nonsecretory
17.	HMPREF0389_00315	Conserved hypothetical protein	70.7	35/0.11	4	C-7.50 EC-0.73	Secretory system-2 pilus domain	–	Nonsecretory
18.	HMPREF0389_00575	Fibronectin-binding protein	68.1	102/0.25	12	C-7.50 EC-0.73	Protein A binding adherence fibronectin/fibrinogen domain	–	Nonsecretory
19.	HMPREF0389_00223	S layer Y containing domain	66.7	651/0.69	22	CW-9.2 EC-0.78	S layer homology domain	1.88	N terminal single peptide

Spot	Accession[a)]	Protein description[a)]	Mol. wt/Calculated mol. wt (kDa)	PMF score[b)]/(emPAI)	Total peptides matched[c)]	PSORT prediction score and category[d)]	Domains[e)]	HI score[f)]	Nature of protein[g)]
20.	HMPREF0389_01573	V-type ATP synthetase alpha chain	66.4	21/0.09	3	C-9.97	ATP-binding V type domain	–	Nonsecretory
21.	HMPREF0389_00803	Conserved hypothetical protein	63.8	30/0.05	4	Unknown	Histidine kinase domain	–	Nonsecretory
22.	HMPREF0389_00261	Conserved hypothetical protein	62.9	17/0.07	4	Unknown	EF-hand calcium-binding domain	–	Nonsecretory
23.	HMPREF0389_00804	Oligopeptide-binding protein	60.25	27/0.07	7	EC-0.91	Lipid attachment domain at two positions	2.26	N terminal signal peptide
24.	HMPREF0389_01605	Formate tetra hydrofolate ligase	60.17	16/0.07	3	C-7.0 EC-0.73	FTH dignature domain	–	Nonsecretory
25.	HMPREF0389_00868	DAK 2 domain protein	58.8	11/0.06	2	C-7.50 EC-0.73	DhaL profile domain	–	Nonsecretory
26.	HMPREF0389_00596	UDP-N-muramyl tripeptide synthetase	57.06	145/0.13	16	C-7.50 EC-0.73	Cell wall tripeptide synthetase domain	–	Nonsecretory
27.	HMPREF0389_00480	Amido transferase family protein	54.7	345/0.54	34	C-7.5 EC-0.73	GATB domain	–	Nonsecretory
28.	HMPREF0389_01130	Ferrous hydrogenase	54.3	32/0.07	3	C-7.5 EC-0.73	Ferrodoxin type Fe-S binding domain	1.88	N terminal signal peptide
29.	HMPREF0389_01374	Conserved hypothetical protein	48.5	52/0.07	6	C-9.5 EC-0.2	YNIH -BH1805-YDJI domain	–	Nonsecretory
30.	HMPREF0389_00504	Peptidase U32 family protein	47.7	22/0.09	7	C-7.50 EC-0.73	Peptidase U 32 domain	–	Nonsecretory
31.	HMPREF0389_01584	Arginine deiminase	46.6	23/0.07	12	C-7.5 EC-0.73	Arginine deiminase domain		Nonsecretory
32.	HMPREF0389_01344	NLP/P60 domain protein	45.4	26/0.07	8	EC-9.60 C-0.15	G5 domain	–	Nonsecretory
33.	HMPREF0389_01570	Acetyl ornithine transaminase	43.5	195/0.44	16	C-9.97 EC0.02	AA transfer class 3 domain	–	Nonsecretory protein
34.	HMPREF0389_00538	Processive diacylglycerol glucosyl transferase	42.2	11/0.05	2	Unknown	MGDG domain	–	Nonsecretory
35.	HMPREF0389_01465	Conserved hypothetical protein	41.5	29/0.13	4	C-7.5 EC-0.73	Hydrolase domain	–	Nonsecretory
36.	HMPREF0389_00744	Butryl coA dehydrogenase	41.25	11/0.07	2	C-7.5 EC-0.73	Acetyl coA DH1 and DH2 domain	–	Nonsecretory
37.	HMPREF0389_00745	Acetyl coA acetyl transfserase	40.9	51/0.07	9	C-7.2 EC-0.93	Thiolase 1,2,3 domain	–	Nonsecretory
38.	HMPREF0389_01008	Membrane lipoprotein	39.54	39/0.06	5	Unknown	N terminal lipoprotein lipid attachment domain	2.31	N terminal signal peptide
39.	HMPREF0389_01567	N acetyl gamma glutamyl phosphate reductase	38.7	79/0.34	13	Unknown	NAC gama glutamyl phosphate domain	–	
40.	HMPREF0389_01445	O-Sialoglycoprotein endo peptidase.	36.6/36.2	22/0.55	5	1.806 C 1.17M 1.17M	Metal-dependent protease-molecular chaperone domain	–0.45	Potent cleavage site without N terminal signal sequence

Spot	Accession[a)]	Protein description[a)]	Mol. wt/Calculated mol. wt (kDa)	PMF score[b)]/(emPAI)	Total peptides matched[c)]	PSORT prediction score and category[d)]	Domains[e)]	HI score[f)]	Nature of protein[g)]
41.	HMPREF0389_00940	Phosphate acetyl transferase	36.0	26/0.11	2	C-7.5 EC-0.73	Acetyl transferase metal binding domain	–	Nonsecretory
42.	HMPREF0389_00704	TRAP transporter solute receptor protein	35.9	344/0.30	16	Unknown	Membrane lipoprotein lipid attachment domain	1.12	N terminal signal peptide
43.	HMPR45EF0389_01401	Conserved hypothetical protein	34.9	30/0.09	6	EC-0.73	Precursor signal YQFA trans membrane domain	3.67	Strong N terminal signal peptide
44.	HMPREF0389_00901	Cobalt import ATP-binding protein	33.92	22/0.08	8	CM-8.79 EC-0.09	CBIO and ATP transporter domain	–	Nonsecretory
45.	HMPREF0389_01198	L-aminopeptidase	33.3	12/0.09	4	C-7.50 EC-0.73	Peptidase DMPA hydrolase domain	–	Nonsecretory
46.	HMPREF0389_01569	Acetyl glutamate kinase	31.03	741/2.34	59	EC-0.73	Arginine amino acid kinase	–	
47.	HMPREF0389_01545	Copper amine oxidase N-domain protein	30.5	22/0.09	6	Unknown	Precursor signal domain	1.96	N terminal signal sequence
48.	HMPREF0389_01619	Iron-sulfur cluster-binding protein	29.1	24/0.51	2	C-7.5 EC-0.73	4Fe-4S-ferredoxin type iron-sulfur binding domain	–	Nonsecretory
49.	HMPREF0389J582	Phosphoglycerate mutase	29.1	45/0.56	7	C-6.23	PGAM domain	–	Nonsecretory
50.	HMPREF0389_00100	Glutamate racemase	29.4	47/0.06	10	EC-0.75 C-3.45	Aspartate glutamate racemase signature	–	
51.	HMPREF0389_01471	Glutaconyl coA decarboxylase	29.4	383/0.22	18	CM	Acetyl CoA CT- N and C terminal domains	–	
52.	HMPREF0389_00119	Pyrroline-5-carboxylate reductase	28.8	10/0.07	2	C-9.95	P5CR domain	–	Nonsecretory
53.	HMPREF0389_00743	Electron transfer flavoprotein beta	28.2	26/0.12	3	EC-0.73 C-6.32	ET-Flavoprotein beta domain	–	
54.	HMPREF0389_01259	Histidinol phosophatase	25.2	36/0.10	3	C-7.50 EC-0.73	PHP-C terminal domain	–	Nonsecretory
55.	HMPREF0389_00321	Conserved hypothetical protein	23.9	21/0.10	4	Unknown	No conserved domain	2.01	N terminal signal peptide
56.	HMPREF0389_00975	TetR family transcriptional regulator	22.8	65/0.12	6	C-7.50 EC-0.73	HTH-TETR-2 domain	–	Nonsecretory
57.	HMPREF0389_01744	Conserved hypothetical protein	22.7	11/0.09	2	C-7.5 EC-0.73	Uncharacterized domain	–	Nonsecretory
58.[h)]	HMPREF0389_01071	Tetracyclin resistant protein	20.8	34/0.11	4	C-7.50 EC-0.73	No conserved domain	–	Nonsecretory
59.[h)]	HMPREF0389_01503	Conserved hypothetical protein	15.7	11/0.07	2	Unknown	No conserved domain	–	Nonsecretory
60.[h)]	HMPREF0389_01654	Neutrophil-activating factor protein A	14/16.2	12/0.07	2	2.310 C 0.099 M	DPS domain	0.32	Nonsecretory
61.[h)]	HMPREF0389_01741	Conserved hypothetical protein	8.7	32/0.07	2	Unknown	No conserved domain	–	Nonsecretory

[a)] Accession numbers and protein descriptions are from the NCBI *F alocis* genome project (http://www.ncbi.nlm.nih.gov/genomeprj/46625).

[b)] Peptide mass fingerprinting score from Mascot.

[c] Number of matched peptides derived from Mascot.

[d] Psortb prediction score classifying protein as: C, cytoplasmic; CM, cytoplasmic membrane; M, membrane; CW, cell wall; PP, periplasm; Ex, extra cellular. Non classical secretory protein in silico prediction through "Secretome."

[e] Conserved domain prediction using the NCBI-Conserved domain database search.

[f] Hydropathy index (HI) score from the iPsort predictions on the nature of protein, high positive score indicate presence of a signal sequence negative scores predict proteins as non secretory.

[g] iPsort prediction showing protein to contain signal sequence, cleavage site and classification of protein to be secretory or nonsecretory.

[h] Low molecular weight protein spots not clearly seen in Fig. 6 but confirmed by MS analysis.

Table 5

Proteases in the genome of *F. alocis*

Name	Annotation
RIP metalloprotease	HMPREF0389_00112
Protease	HMPREF0389_00122
ATP-dependent protease La	HMPREF0389_00279
Zinc protease	HMPREF0389_00298
ATP-dependent zinc metalloprotease FtsH	HMPREF0389_01001
Caax amino protease family protein	HMPREF0389_00677
Caax amino protease	HMPREF0389_00590
Metalloprotease	HMPREF0389_00692
Glycoprotease family protein	HMPREF0389_01443
Xaa pro dipeptidase	HMPREF0389_01538
O-sialoglycoprotein endopeptidase	HMPREF0389_01445
Serine protease HtrA	HMPREF0389_01460
ATP-dependent Clp protease	HMPREF0389_01648
Carboxy-processing protease	HMPREF0389_00522
Oligoendopeptidase F	HMPREF0389_00926 HMPREF0389_00527

Table 6

Proteome profiling and categorization of various fractions of *F. alocis* strains

Strains and fractions	Protein classification									
	Protease/ peptidases	Lipo proteins	Protein metabolism	Hypothetical protein	Energy metabolism	Protein secretory pathways	Transport and binding proteins	Antitoxin and antigens	DNA metabolism	Regulatory protein
ATCC–MEMBRANE FRACTION	2	1	11	11	5	2	4	1	3	4
D-62D–MEMBRANE FRACTION	8	1	8	10	5	1	7	2	3	5
ATCC–EXTRA CELLULAR FRACTION	4	1	8	14	6	1	4	0	3	8
D-62D–EXTRA CELLULAR FRACTION	6	1	16	15	7	2	8	3	5	8

Table 7
Genome-wide survey of *F. alocis* cell wall anchored proteins

Features	*F. alocis* ATCC strain (*n* = 50)	*F. alocis* D-62D strain (*n* = 56)
Export features		
Signal sequence [a)]	5	14
Signal peptidase I cleavage[b)]	4	9
Transmembrane helix domain [c)]	7	15
Cell wall anchored proteins		
N or C-terminally anchored proteins [d)]	8	10
Sortase A. *LP×TG* anchors [e)]	–	2
Atypical sortase anchors [e)]	1	3
Sortase B motif [e)] *NP(Q/K)(T/S)(N/G/S)(D/A)*	1	–
Sortase D motif [e)] *LP×TA*	–	1
Peptidoglycan-binding domains [f)]	10	20
LysM domains [g)]	2	4
Lipoprotein anchors [h)]	–	2
GW repeats [i)]	5	10
WxL domains [j)]	3	6
Glycin-rich C terminal motif [k)]	–	25

[a)] Signal sequence prediction was done with the hidden Markov model in SignalP3.0 [28], with *p* values of > 0.95 as the cutoff.

[b)] Cleavage site prediction was done with the neural network model in SignalP3.0, with $\mathbf{C}_{max}$ values of > 0.52 and $\mathbf{Y}_{max}$ values of > 0.32 as cutoffs.

[c)] TMMH prediction was made using SignalP3.0 [28].

[d)] The N terminal and C terminal domains were identified using the HMM.

[e)] LPXTG anchors, atypical sortase anchors, sortase D motifs were predicted by the hidden Markov model for sortase substrates [32].

[f)g)] From the Pfam database, with a cutoff E value of $\leq 10^{-5}$.

[h)] Lipoprotein prediction was done as described by Sutcliffe and Harrington [31].

[i)] Manual screening for the presence of GW residues in repetitive regions was performed.

[j)] Prediction based on the presence of the [LI]TW[TS]L motif in the C-terminal sequence.

[k)] Sequence alignment and C terminal motif identifications were made using MEGA version 4.0 [25].